[Short title + Author Name - P&H title] 17 (2024) 105423

Contents lists available at ScienceDirect

Arabian Journal of Chemistry

journal homepage: www.ksu.edu.sa

Structure-based design, synthesis and biological evaluation of N-substituted 6H-thiochromeno[2,3–c]quinolin-12(12H)-one as potential breast cancer drugs

Maryam Rachmawati Sumitra [a,b], Lung-Ching Chen [c,d], Wei-Chen Tsai [e], Muhamad Ansar [f], Bashir Lawal [a,b], Ntlotlang Mokgautsi [a,b], Jih-Hwa Guh [j], Alexander T.H Wu [g,h,i,*], Hsu-Shan Huang [a,b,e,i,k,*]

[a] PhD Program for Cancer Molecular Biology and Drug Discovery, College of Medical Science and Technology, Taipei Medical University, Taipei 11031, Taiwan
[b] Graduate Institute of Cancer Biology and Drug Discovery, College of Medical Science and Technology, Taipei Medical University, Taipei 11031, Taiwan
[c] Division of Cardiology, Department of Internal Medicine, Shin Kong Wu Ho-Su Memorial Hospital, Taipei 11101, Taiwan
[d] School of Medicine, Fu Jen Catholic University, New Taipei 24205, Taiwan
[e] School of Pharmacy, National Defense Medical Center, Taipei 11490, Taiwan
[f] Clinical Drug Development of Herbal Medicine, Taipei Medical University, Taipei 11031, Taiwan
[g] The PhD Program of Translational Medicine, College of Science and Technology, Taipei Medical University, Taipei 11031, Taiwan
[h] Clinical Research Center, Taipei Medical University Hospital, Taipei Medical University, Taipei 11031, Taiwan
[i] Graduate Institute of Medical Sciences, National Defense Medical Center, Taipei 11490, Taiwan
[j] School of Pharmacy, National Taiwan University, No. 33, Linsen S. Rd., Zhongzheng Dist., Taipei 10025, Taiwan
[k] Biotechnology Research and Development, College of Pharmacy, Taipei Medical University, Taipei 11031, Taiwan

ARTICLE INFO

Keywords:
Breast cancer
NCI 60-cell panel assay
Molecular docking
Tetraheterocyclic

ABSTRACT

Tetraheterocyclic compounds, derived from natural sources and contemporary pharmaceuticals, have shown promise as multitarget therapeutic agents. However, their mechanisms of action remain partially understood. In this study, we synthesized a series of 6H-thiochromeno[2,3-c]quinolin-12(12H)-one derivative, totaling 26 compounds, and assessed their potential for therapeutic application. We evaluated their effects on cell proliferation and conducted NCI-60 cell panel assays. MTT assays revealed that select compounds exhibited notable antiproliferative activity against two breast cancer cell lines (MCF-7 and MDA-MB-468). Notably, compounds **17** and **18** displayed the highest cytotoxicity against these cell lines. Furthermore, one-dose assays of the NCI-60 human tumor cell line screening program identified compounds **6**, **7**, **16**, **18**, **20**, **24**, **25**, and **30** for further investigation.

Subsequent five-dose cytotoxicity studies focused on compounds **18** and **20**, which met the threshold inhibition criteria across a panel of cell lines. Our study highlights the effectiveness of compounds **18** and **20** in targeting breast cancer cell lines. Molecular docking simulations revealed that these compounds bind to the active sites of topoisomerase I (TOPO I). Our findings suggest that these novel compounds are promising anticancer agents, particularly against breast cancer, and are worthy of consideration as lead pharmacological candidates.

1. Introduction

Breast cancer is the second most prevalent and leading cause of cancer deaths in women globally (Siegel, 2023; Fares et al., 2023). Based on molecular biological techniques and gene expression profiles, breast cancer can be classified into five clinical characteristics and treated depending on whether estrogen receptor (ER)-, progesterone receptor (PR)-, or human epidermal growth factor receptor (HER)-2-positive, respectively (Orrantia-Borunda et al., 2022; Tang, 2018). Despite the exploitation of genes and immunotherapy, chemotherapy is still the

Peer review under responsibility of King Saud University.
* Corresponding authors.
E-mail addresses: chaw1211@tmu.edu.tw (A.T.H Wu), huanghs99@tmu.edu.tw (H.-S. Huang).

https://doi.org/10.1016/j.arabjc.2023.105423
Received 24 September 2023; Accepted 30 October 2023
Available online 2 November 2023

most effective strategy in clinical practice for most cancer patients. In addition, DNA topoisomerases are essential enzymes that manipulate the topology of DNA in cells and play essential roles in DNA replication, transcription, chromosome segregation, and recombination (McKie et al., 2021). Topoisomerase inhibitors are still widely used as first-line anticancer drugs due to their high activity and high expression in tumor cells. Natural product-derived agents have greatly contributed to the development of novel treatments for cancer, such as camptothecin (Ghanbari-Movahed et al., 2021), topotecan (Jaeckle et al., 2020), and irinotecan (Wang et al., 2020), are classical topoisomerase inhibitors (Fig. 1). Targeting of the topoisomerase for cancer research continues to be a highly active area of the development of new anticancer drugs, especially in breast cancer (Hevener et al., 2018).

Accordingly, many small active molecules with different chemical scaffolds have emerged as small molecule inhibitors. Single-targeted chemotherapy strategies are often hampered by limited efficacy, toxic side effects, and drug resistance (Min and Lee, 2022). Multitarget therapeutics have become a popular area that can act on two or more targets simultaneously, with better therapeutic advantages and potentially synergistic effects (Raevsky, 2018; Zhong et al., 2021). Although multitarget small-molecule inhibitors have several different mechanisms of action, this therapy still faces issues, such as drug resistance and undesirable side effects, which need to be resolved for their application to breast cancer treatment (Liu et al., 2020; Yuan et al., 2020).

As part of our ongoing efforts to develop potent and selective small molecule inhibitors for cancer therapy, we have employed a computational fragment-based drug discovery (FBDD) method to obtain a series of tetraheterocyclic derivatives because of their adaptability and distinctive qualities in different biological and medicinal applications (Abdella et al., 2020; Jampilek, 2019). Although heterocyclic anthracycline and its derivatives are well-known drugs with several therapeutic applications, their pharmacological characteristics can still be improved (Karthikeyan et al., 2023; Martins-Teixeira and Carvalho, 2020).

The innovation in our approach lies in our efforts to deliver multitarget therapies that can simultaneously address multiple critical cellular processes involved in cancer progression. This strategy aims to enhance treatment efficacy and minimize drug resistance, offering a potential breakthrough in breast cancer therapy. In our previous study, compound **11** (NSC763967), which contains thiadiazoles, was discovered to have broad-spectrum cytotoxicity against several cancer cells among our collection of small-molecule inhibitors. However, our candidate exhibited promising results, which may reveal important details about the cytotoxic, cytostatic, and selectivity characteristics of cells (Ali et al., 2021). Additionally, significant attention has been paid to developing techniques that lower the toxicity of parent compounds of anthracycline derivatives, such as metixene (Fares et al., 2023), xanthones (Kurniawan et al., 2021), and thioxanthones (Lima et al., 2018) (Fig. 1). In addition to our ongoing efforts to develop potent and selective small-molecule inhibitors for cancer therapy, we have explored quinoline, a unique and promising chemical scaffold in our research (Abdolmohammadi et al., 2020). Quinoline is a chemical building block of a large number of heterocyclic compounds with a broad range of biological and pharmacological properties such as antibacterial (Bakır and Lawag, 2020), antimicrobial (Senerovic, 2020), antitumor (Lauria et al., 2021; El Rhabori et al., 2022; Iqbal et al., 2019), and anti-HIV (Chokkar et al., 2019). These promising results encouraged us to identify the most favorable chemical modifications based on our previous candidate, which is required for the development of novel drugs with potential applications in cancer therapy.

Herein, we designed and synthesized a novel series of compounds based on the 6H-thiochromeno[2,3–c] quinoline-12 (12H)-one scaffold using different N-substitutions on the 3-position as depicted in Scheme 1. Their cytotoxicity against two human breast cancer cell lines (MCF7 and MDA-MB-468) using MTT assays is assessed (Table 1). Moreover, compounds **6** (NSC784437), **7** (NSC784438), **16** (NSC784445), **18** (NSC784447), **20** (NSC784449), **24** (NSC784440), **25** (NSC784442), **28** (NSC784441), and **30** (NSC784444) were tested by the NCI, using single-dose cytotoxicity experiments against a panel of 60 human cancer cell lines (Table 2). All these results characterize **18** (NSC784447) and **20** (NSC784449) satisfied the predetermined threshold of growth-inhibition criteria of the NCI. Accordingly, they were evaluated using cytotoxicity studies with five doses against a panel of 60 cancer cell lines (Table 3). We discovered these two compounds had significant multi-log differential activity patterns, with 50 % growth inhibition (GI_{50}) values against several cancer cell lines in the sub-micromolar range (Table 3).

Using comparative correlations of the cytotoxic activities of drugs featured in the NCI database, we performed COMPARE analytical studies to identify compounds with similar targets and mechanisms of action to our test compounds and gain insights into potential targets and

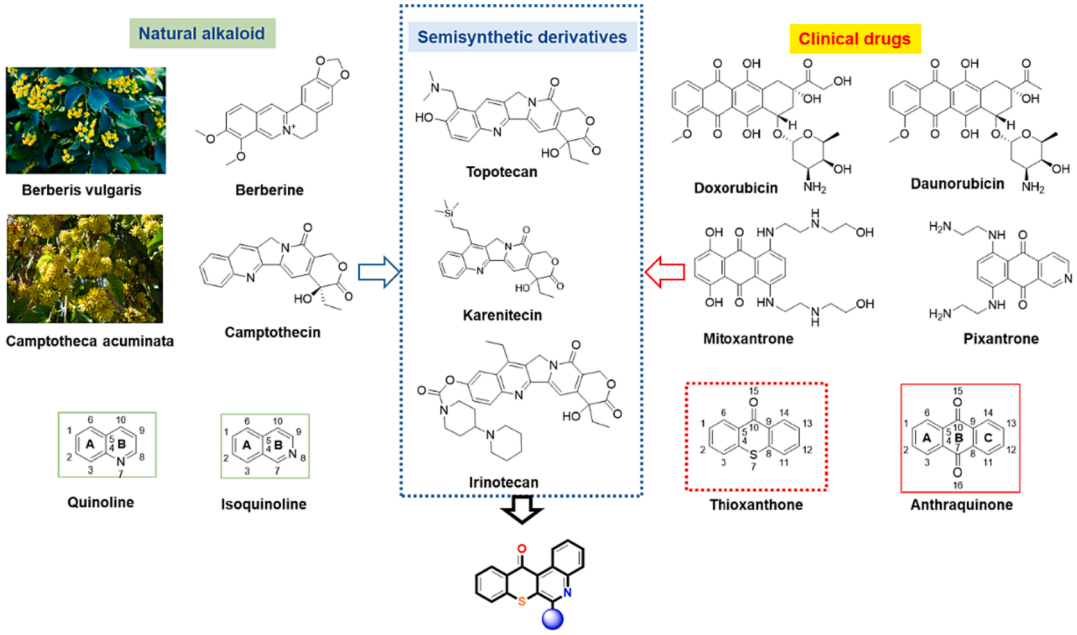

Fig. 1. Rational design of 6H-thiochromeno[2,3-c] quinoline-12 (12H)-one derivatives as anticancer drugs.

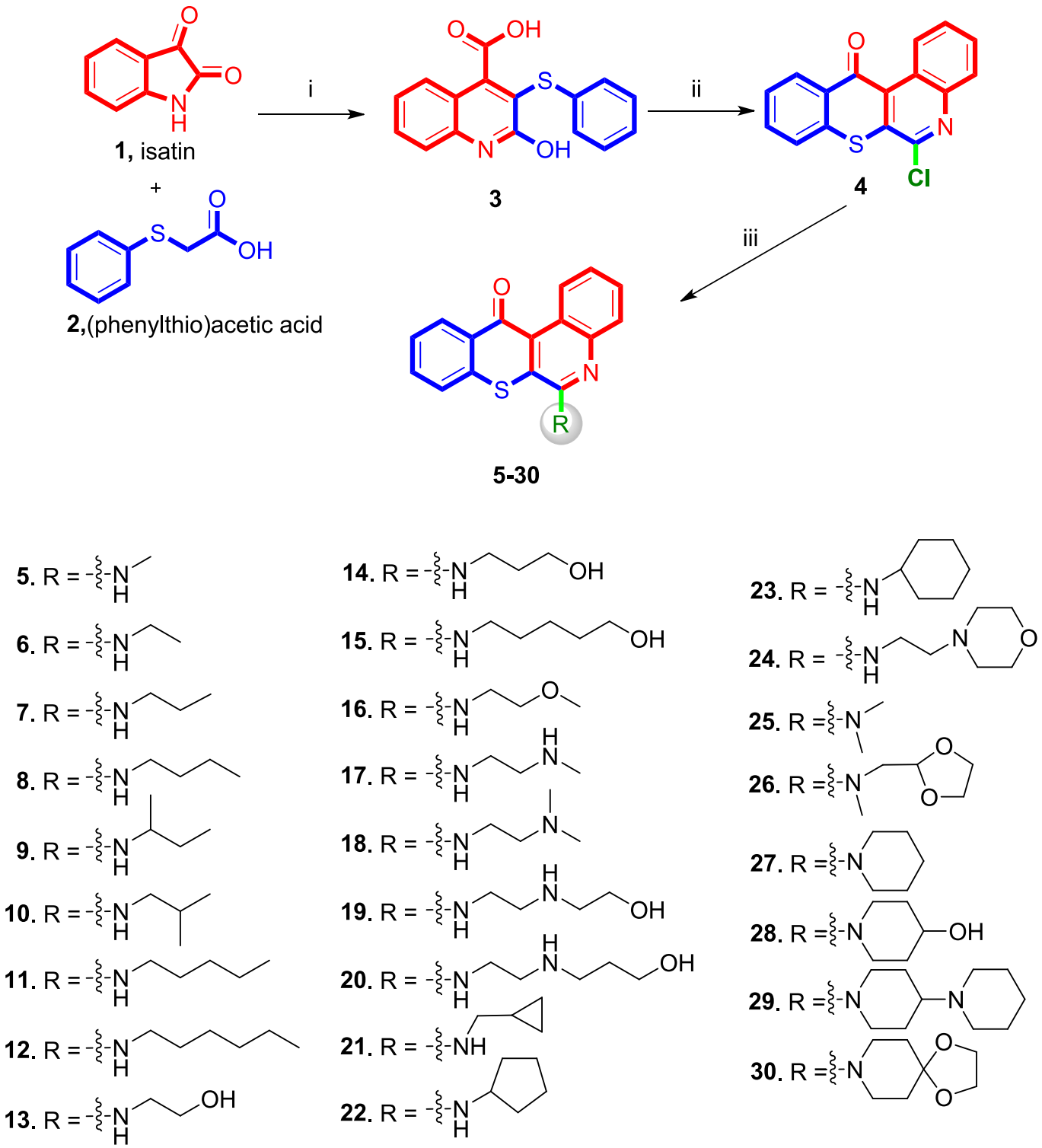

Scheme 1. Synthesis routes of 6H-thiochromeno [2,3-c] quinolin-12(12H)-one derivatives. Reagents and conditions: (i) NaOAc, 150 °C, 1 h; (ii) POCl3, 150 °C, 48 h; (iii) DMSO, appropriate secondary amines, Na_2CO_3, 150 °C, 10 h.

mechanisms of our drugs (Haji et al., 2023). We discovered that certain inhibitors, including aurora kinase A (AURKA), poly(ADP ribose) polymerase (PARP), cyclin-dependent kinase (CDK) 4/6, and topoisomerase (TOPO) I and II, were strongly correlated with the cytotoxic profiles of **18** (NSC784447) and **20** (NSC784449). Additionally, based on our molecular modeling investigations, we discovered that compounds **18** (NSC784447) and **20** (NSC784449) are effective TOPO-1 inhibitors. As shown in this publication, our data present a novel series of potential multitarget anticancer drugs that represent interesting candidates for further therapeutic development.

Table 1
Cytotoxic effects of compounds **5**–**30** on the MCF-7 and MDA-MB-468 human breast cancer cell lines as detected by an MTT assay.

No.	R substitutions	MTT assay		No.	R substitutions	MTT assay	
		MCF-7 (μM)	MDA-MB-468 (μM)			MCF-7 (μM)	MDA-MB-468 (μM)
5		2.99 ± 0.35	1.84 ± 0.33	**19**	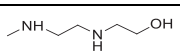	3.68 ± 0.49	2.6 ± 0.07
6		> 20	> 20	**20**	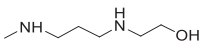	3.5 ± 0.19	2.97 ± 0.29
7		> 20	> 20	**21**		18.35 ± 1.18	> 20
8		> 20	> 20	**22**	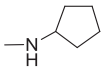	> 20	> 20
9		> 20	2.65 ± 0.11	**23**	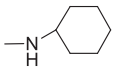	> 20	2.3 ± 0.28
10		> 20	2.46 ± 0.13	**24**	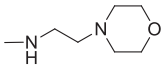	19.29 ± 1.24	2.45 ± 0.27
11	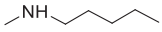	> 20	> 20	**25**		> 20	> 20
12	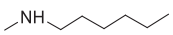	> 20	> 20	**26**	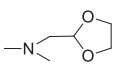	> 20	> 20
13	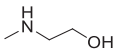	> 20	> 20	**27**		> 20	> 20
14	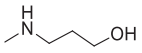	> 20	> 20	**28**	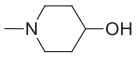	> 20	> 20
15	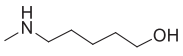	> 20	2.72 ± 0.04	**29**	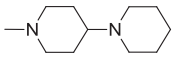	> 20	> 20
16	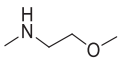	> 20	> 20	**30**	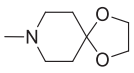	> 20	> 20
17	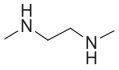	2.3 ± 0.28	2.07 ± 0.57	–	Doxorubicin	0.41 ± 0.01	1.96 ± 0.52
18	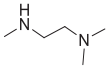	2.94 ± 0.19	2.5 ± 1.3	–	Camptothecin	0.54 ± 0.11	2.23 ± 0.32

Table 2
Selectivity index (SI) analysis was performed on the antiproliferative sensitivities of TC-S-1 derivatives.

Compound	Cell lines			
	MCF-7		MDA-MB-468	
	IC_{50} (μM)	Selectivity index [b]	IC_{50} (μM)	Selectivity index [b]
5	2.99	1.93	1.84	1.30
17	2.3	2.51	2.07	1.16
18	2.94	1.96	2.5	0.96
19	3.68	1.57	2.6	0.92
20	3.5	1.65	2.97	0.80
24	19.29	0.29	2.45	0.98
Total mean [a]	5.78		2.40	

[a] The total mean 50 % inhibitory concentration (IC_{50}) value of all active compounds in μM. [b]Selectivity index (SI) = total mean/IC_{50} of each compound.

2. Material and methods

2.1. Chemistry

2.1.1. General experimental procedures

All reagents and solvents were purchased from Merck (Germany) and Sigma-Aldrich (USA) and were used without further purification. All reactions were monitored using precoated silica gel 60 F254 (Merck), and thin-layer chromatography (TLC) plates were observed under UV light. Melting points were determined with a Büchi Melting Point B-545 apparatus (National Defense Medical Center, Taiwan). 1H nuclear magnetic resonance (NMR) spectra were recorded using GEMINI300 MHz (National Defense Medical Center, Taiwan) and AM-500 MHz (Bruker) instruments. Chemical shift (d) values were in ppm ranges relative to tetramethylsilane (TMS) as an internal standard. Mass spectra were obtained by Finnigan (National Taiwan University, Taiwan) MAT 95 XL high-resolution mass spectroscopy (HRMS) and Finnigan/Thermo Quest MAT HRMS. Typical experiments illustrating the general procedures for preparing the anthraquinone derivatives are described below.

Table 3
Physicochemical properties, Lipophilicity, Drug-likeness, and Medicinal Chemistry compound **5**, **17**, **18**, **19**, **20**, **21**, **24**, doxorubicin and camptothecin.

Compound	Physicochemical Properties				Lipophilicity and Water Solubility			Drug likeliness			Medicinal chemistry	
	M.W	HBA	HBD	TPSA	XLOGP3	Consensus Log $P_{o/w}$	Log *S*	Lipinski's rules	Veber's rules	Ghose's rules	PAINS	Synthetic accessibility
5	292.35	2	1	70.23	4.09	3.68	−4.80	Yes	Yes	Yes	0 alert	2.84
17	335.42	3	2	82.26	3.66	3.52	−4.52	Yes	Yes	Yes	0 alert	3.12
18	349.45	3	1	73.47	4.13	3.74	−4.88	Yes	Yes	Yes	0 alert	3.23
19	365.45	4	3	102.49	2.97	3.06	−4.09	Yes	Yes	Yes	0 alert	3.20
20	379.48	4	3	102.49	3.88	3.49	−4.67	Yes	Yes	Yes	0 alert	3.28
21	332.42	2	1	70.23	4.83	4.41	−5.30	Yes	Yes	Yes	0 alert	2.98
24	391.49	4	1	82.70	3.75	3.59	−4.84	Yes	Yes	Yes	0 alert	3.35
Doxorubicin	543.52	12	6	206.07	1.27	0.44	−3.91	No	No	No	1 alert	5.81
Camptothecin	348.35	5	1	81.42	1.74	2.20	−3.49	Yes	Yes	Yes	0 alert	3.84

2.1.1.1. General method for synthesis of compound 3. A mixture of isatin (**1**) (0.44 g, 2.99 mmol), (phenylthio)acetic acid (**2**) (0.78 g, 4.64 mmol), and sodium acetate (0.05 g) was heated to 150 °C in a miniclave for 1 h monitored by TLC (Thin Layer Chromatography). After cooling, 10 mL of acetic acid was added to the mixture, and the gray precipitate was collected and washed with acetic acid, water, and n-hexane to obtain a light-purple compound (**3**).

2.1.1.2. General method for synthesis of compound 4. A mixture of compound **3** (84 mol) and $POCl_3$ (200 mL) was heated to 150 °C for 48 h. After the reaction was complete, the mixture was cooled to room temperature and poured into a water bath at 0 °C. It was then filtered by suction to collect a green precipitate, and the precipitate was added to a 10 % $NaHCO_3$ solution (50 mL) and stirred for 1 h. The precipitate was collected and washed with water. The crude product was recrystallized in dichloromethane to give a yellowish product (**4**).

2.1.1.3. General method for synthesis of compounds 5-30. Method 1: Preparation of compounds **5, 7–12, 16**, **21**, **23**, **25**, **28**, and **29**.

A mixture of compound **4** (2 mmol), alkylamine, and sodium carbonate (2.5 mmol) was dissolved in DMSO (9 mL) and heated in a miniclave (to 150 °C) for 2 h. After the reaction was completed, the mixture was poured into water (250 mL) and allowed to stand for about 5–10 min. At this time, a yellow precipitate had precipitated out. The precipitate was collected by suction and filtered. The precipitate was recrystallized with dichloromethane to obtain compounds **5, 7–12, 16**, **21**, **23**, **25**, **28**, and **29**.

Method 2: Preparation of compounds **6, 13–15, 17–19**, **22**, **24**, **26**, **27**, and **30**.

A mixture of compound **4** (1 mmol), alkylamine, and sodium carbonate (1.5 mmol) in DMSO (8 mL) was refluxed for 4 h. After the reaction was completed, the mixture was poured into water (250 mL) and filtered to collect the resulting precipitate. The precipitate was extracted with dichloromethane and water to collect the organic material. The layers were concentrated and drained under reduced pressure. The precipitate was recrystallized with dichloromethane to afford compounds **6, 13 ~ 15, 17–19**, **22**, **24**, **26**, **27**, and **30**.

Method 3: Preparation of compound **20**.

To a solution of compound **4** (2 mmol) in DMSO was added alkylamine and sodium carbonate (2.5 mmol), and then the mixture was refluxed for 6 h (at 100 °C). After the reaction was completed, the material was poured into 250 mL of water. The precipitate appeared at this time and was filtered to collect the precipitate. The crude precipitate was purified by column chromatography (hexane: dichloromethane 1:1) to afford compound **20**.

2.1.1.3.1. 2-hydroxy-3-(phenylthio)quinoline-4-carboxylic acid (3). The pure compound was obtained as a purple solid (yield 86 %), $R_f = 0.8$ at MeOH, Mp 304–305 °C. ^{1}H NMR (400 MHz, DMSO-d_6): δ (ppm) 7.16–7.32 (6H, m), 7.38 (1H, d, $J = 8.4$ Hz), 7.45 (1H, d, $J = 8.4$ Hz), 7.61 (1H, t, $J = 8.4$ Hz), 12.20 (1H, s). ^{13}C NMR (100 MHz, DMSO-d_6): δ (ppm) 115.17, 115.78, 120.26, 122.73, 125.74, 126.28, 128.05, 128.97, 132.00, 134.84, 139.64, 151.18, 159.07, 166.44. HRMS (ESI) *m/z* calcd. for $C_{16}H_{11}NO_3S^+$ $[M]^+$: 297.0460; found $[M + H]^+$: 298.0520, $[M + Na]^+$: 320.0340, $[M-H]^+$: 296.0392.

2.1.1.3.2. 6-chloro-12H-thiochromeno[2,3–c]quinolin-12-one (4). The pure compound was obtained as a yellow solid (yield 74 %), $R_f = 0.8$ at CH_2Cl_2, Mp 212–213 °C. ^{1}H NMR (400 MHz, DMSO-d_6): δ (ppm) 7.74 (1H, t, $J = 8$ Hz), 7.85–7.92 (3H, m), 8.08–8.11 (2H, m), 8.49 (1H, dd, $J = 8$, 0.8 Hz), 9.62 (1H, dd, $J = 8.4$, 1.6 Hz). ^{13}C NMR (100 MHz, DMSO-d_6): δ (ppm) 124.92, 126.39, 127.43, 128.81, 129.25, 129.57, 130.34, 130.63, 130.84, 131.49, 133.76, 134.44, 144.94, 146.79, 181.52, 166.44. HRMS (ESI) *m/z* calcd. for $C_{16}H_7ClNOS^+$ $[M]^+$: 295.9931; found $[M + H]^+$: 298.0088, $[M + H + 2]^+$: 300.0063.

2.1.1.3.3. 6-(Methylamino)-12H-thiochromeno[2, 3-c]quinolin-12-one (5). Compound **5** was prepared from **4** and methylamine (20 mmol). The compound was obtained in a 71 % yield, $R_f = 0.2$ at CH_2Cl_2, Mp 184–186 °C. ^{1}H NMR (400 MHz, DMSO-d_6): δ (ppm) 3.24 (3H, d, $J = 4.4$ Hz), 4.94 (1H, s), 7.43 (1H, t, $J = 7.2$ Hz), 7.54–7.66 (4H, m), 7.84 (1H, d, $J = 8.4$ Hz), 8.56 (1H, d, $J = 8$ Hz), 9.46 (1H, d, $J = 8.8$ Hz). ^{13}C NMR (100 MHz, DMSO-d_6): δ (ppm) 29.35, 120.89, 123.88, 124.45, 125.95, 126.01, 127.09, 127.62, 129.29, 129.76, 129.98, 131.65, 132.10, 132.84, 145.60, 151.38, 182.18. HRMS (ESI) *m/z* calcd. for $C_{17}H_{11}N_2OS^+$ $[M]^+$: 291.0587; found $[M + H]^+$: 293.0744.

2.1.1.3.4. 6-(Ethylamino)-12H-thiochromeno[2, 3-c]quinolin-12-one (6). Pure compound **6** was prepared from **4** and ethylamine (10 mmol). The compound was obtained as a yellow solid (yield 83 %), $R_f = 0.3$ at CH_2Cl_2, Mp 162–163 °C. ^{1}H NMR (400 MHz, DMSO-d_6): δ (ppm) 1.41 (3H, t, $J = 7.2$ Hz), 3.75 (2H, sep, $J = 4.4$ Hz), 4.84 (1H, s), 7.43 (1H, td, $J = 8.4$, 1.2 Hz), 7.55–7.68 (4H, m), 7.82 (1H, d, $J = 8.4$ Hz), 8.57 (1H, d, $J = 8$ Hz), 9.46 (1H, dd, $J = 8.4$ Hz, 1.2 Hz). ^{13}C NMR (100 MHz, DMSO-d_6): δ (ppm) 14.80, 37.32, 120.84, 123.70, 124.35, 125.92, 125.97, 127.09, 127.58, 129.22, 129.73, 129.97, 131.60, 132.08, 132.86, 145.62, 150.69, 182.19. HRMS (ESI) *m/z* calcd. for $C_{18}H_{13}N_2OS^+$ $[M]^+$: 305.0743; found $[M + H]^+$: 307.0895.

2.1.1.3.5. 6-(Propylamino)-12H-thiochromeno[2, 3-c]quinolin-12-one (7). Compound **7** was prepared from **4** and propylamine (6 mmol). The compound was obtained in a 69 % yield, $R_f = 0.37$ at CH_2Cl_2, Mp 133–134 °C. ^{1}H NMR (400 MHz, DMSO-d_6): δ (ppm) 1.09 (3H, d, $J = 7.6$ Hz), 1.75–1.85 (2H, m), 3.65–3.70 (2H, m), 4.88 (1H, t, $J = 4.8$ Hz), 7.41 (1H, t, $J = 7.2$ Hz), 7.53–7.66 (4H, m), 7.81 (1H, dd, $J = 8$ Hz, 0.8 Hz), 8.55 (1H, dd, $J = 8.4$ Hz, 1.2 Hz), 9.45 (1H, dd, $J = 8.8$ Hz, 1.2 Hz). ^{13}C NMR (100 MHz, DMSO-d_6): δ (ppm) 11.69, 22.65, 44.09, 120.81, 123.73, 124.29, 125.90, 125.94, 127.06, 127.54, 129.20, 129.68, 129.92, 131.54, 132.04, 132.81, 145.59, 150.75, 182.15. HRMS (ESI) *m/z* calcd. for $C_{19}H_{15}N_2OS^+$ $[M]^+$: 319.0900; found $[M + H]^+$: 321.1057.

2.1.1.3.6. 6-(Butylamino)-12H-thiochromeno[2, 3-c]quinolin-12-one (8). Compound **8** was prepared from **4** and n-butylamine (5 mmol). The compound was obtained in a 69 % yield, $R_f = 0.43$ at CH_2Cl_2, Mp 104–106 °C. ^{1}H NMR (400 MHz, DMSO-d_6): δ (ppm) 0.94 (3H, t, $J = 7.6$ Hz), 1.40 (2H,$J = 7.6$ Hz), 1.69 (2H, quin, $J = 7.2$ Hz, –CH2-), 3.58 (2H, q, $J = 6.4$ Hz, –CH2-), 7.08 (1H, t, $J = 5.2$ Hz), 7.34 (1H, td, $J = 7.2$ Hz,

1.2 Hz), 7.57 (1H, t, $J = 8.4$ Hz), 7.67 (2H, t, $J = 7.2$ Hz), 7.82 (1H, t, $J = 8.4$ Hz), 7.91 (1H, d, $J = 8$ Hz), 8.45 (1H, d, $J = 8$ Hz), 9.34 (1H, d, $J = 8.8$ Hz). ^{13}C NMR (100 MHz, DMSO-d_6): δ (ppm) 13.98, 20.37, 31.57, 42.07, 120.83, 123.73, 124.31, 125.92, 125.98, 127.08, 127.59, 129.23, 129.75, 130.00, 131.63, 132.08, 132.86, 145.64, 150.78, 182.21. HRMS (ESI) *m/z* calcd. for $C_{20}H_{17}N_2OS^+$ [M]+: 333.1056; found [M + H]$^+$: 335.1212.

2.1.1.3.7. 6-(sec-butylamino)-12H-thiochromeno[2, 3-c]quinolin-12-one (9). Compound **9** was prepared from **4** and *sec*-butylamine (5 mmol). The compound was obtained in a 35 % yield, R_f = 0.53 at CH_2Cl_2, Mp 139–141 °C. ^{1}H NMR (400 MHz, DMSO-d_6): δ (ppm) 1.05 (3H, t, $J = 7.2$ Hz), 1.36 (3H, d, J = 6.4), 1.67–1.80 (2H, m), 4.46–4.52 (1H, m), 4.72 (1H, d, $J = 7.2$ Hz), 7.42 (1H, t, $J = 8.4$ Hz), 7.56–7.63 (2H, m), 7.66 (2H, d, $J = 4$ Hz), 7.81 (1H, dd, $J = 8.4$ Hz), 8.58 (1H, d, $J = 8$ Hz), 9.46 (1H, dd, $J = 8.8$ Hz, 1.2 Hz). ^{13}C NMR (100 MHz, DMSO-d_6): δ (ppm) 10.39, 20.28, 29.57, 48.66, 120.69, 123.68, 124.15, 125.88, 125.90, 127.08, 127.52, 129.14, 129.67, 129.98, 131.53, 132.02, 132.80, 145.65, 150.20, 182.19. HRMS (ESI) *m/z* calcd. for $C_{20}H_{17}N_2OS^+$ [M]$^+$: 333.1056; found [M + H]$^+$: 365.1324.

2.1.1.3.8. 6-(Isobutylamino)-12H-thiochromeno[2, 3-c]quinolin-12-one (10). Compound **10** was prepared from **4** and isobutylamine (5 mmol). The compound was obtained in a 67 % yield, R_f = 0.4 in CH_2Cl_2, Mp 151–153 °C. ^{1}H NMR (400 MHz, DMSO-d_6): δ (ppm) 1.09 (6H, d, $J = 6.4$ Hz), 2.11 (1H, sep, $J = 6.8$ Hz), 3.57 (2H, t, $J = 5.6$ Hz), 4.98 (1H, t, $J = 4.8$ Hz), 7.42 (1H, td, $J = 7.2$, 1.2 Hz), 7.57–7.63 (2H, m), 7.67 (2H, d, $J = 3.6$ Hz), 7.82 (1H, d, $J = 8.4$ Hz), 8.59 (1H, d, $J = 8$ Hz), 9.46 (1H, dt, $J = 8.8$ Hz, 0.8 Hz). ^{13}C NMR (100 MHz, DMSO-d_6): δ (ppm) 20.48, 28.15, 49.65, 120.78, 123.71, 124.24, 125.87, 125.91, 127.02, 127.52, 129.17, 129.66, 129.92, 131.51, 132.02, 132.75, 145.54, 150.78, 182.12. HRMS (ESI) *m/z* calcd. for $C_{20}H_{17}N_2OS^+$ [M]$^+$: 333.1056; found [M + H]$^+$: 335.1212.

2.1.1.3.9. 6-(Pentylamino)-12H-thiochromeno[2, 3-c]quinolin-12-one (11). Compound **11** was prepared from **4** and amylamine (4.5 mmol). The compound was obtained in a 69 % yield, R_f = 0.4 in CH_2Cl_2, Mp 105–107 °C. ^{1}H NMR (400 MHz, DMSO-d_6): δ (ppm) 0.96 (3H, t, $J = 6.8$ Hz), 1.41–1.51 (4H, m), 1.77(2H, quint, $J = 7.2$ Hz), 3.68 (2H, q, $J = 6.4$ Hz), 4.85 (1H, t, $J = 4.8$ Hz), 7.41 (1H, t, $J = 8$ Hz), 7.52–7.65 (4H, m), 7.80 (1H, dd, $J = 8.4$, 0.4 Hz), 8.54 (1H, d, $J = 8.4$ Hz), 9.45 (1H, dd, $J = 8.8$, 0.8 Hz). ^{13}C NMR (100 MHz, DMSO-d_6): δ (ppm) 14.06, 22.49, 29.08, 29.33, 42.32, 120.77, 123.71, 124.24, 125.88, 125.90, 127.03, 127.50, 129.15, 129.64, 129.86, 131.50, 132.00, 132.79, 145.58, 150.70, 182.10. HRMS (ESI) *m/z* calcd. for $C_{21}H_{19}N_2OS^+$ [M]$^+$: 347.1213; found [M + H]$^+$: 349.1369.

2.1.1.3.10. 6-(Hexylamino)-12H-thiochromeno[2, 3-c]quinolin-12-one (12). Compound **12** was prepared from **4** and hexylamine (4 mmol). The compound was obtained in a 96 % yield, R_f = 0.47 in CH_2Cl_2, Mp 89–91 °C. ^{1}H NMR (400 MHz, DMSO-d_6): δ (ppm) 0.93 (3H, t, $J = 6.8$ Hz), 1.33–1.42 (4H, m), 1.49 (2H, quin, $J = 7.2$ Hz), 1.76 (2H, quin, $J = 7.2$ Hz), 3.68 (2H, q, $J = 6.4$ Hz), 4.84 (1H, t, $J = 4.8$ Hz), 7.41 (1H, t, $J = 8$ Hz), 7.52–7.64 (4H, m), 7.80 (1H, dd, $J = 8$, 0.8 Hz), 8.54 (1H, d, $J = 8.4$ Hz), 9.45 (1H, dd, $J = 8.4$, 0.8 Hz). ^{13}C NMR (100 MHz, DMSO-d_6): δ (ppm) 14.09, 22.64, 26.87, 29.37, 31.63, 42.38, 120.79, 123.74, 124.25, 125.90, 125.92, 127.05, 127.51, 129.17, 129.65, 129.86, 131.50, 132.01, 132.81, 145.59, 150.72, 182.11. HRMS (ESI) *m/z* calcd. for $C_{22}H_{21}N_2OS^+$ [M]$^+$: 361.1369; found [M + H]$^+$: 363.1531.

2.1.1.3.11. 6-(2-hydroxyethylamino)-12H-thiochromeno[2, 3-c]quinolin-12-one (13). Compound **13** was prepared from **4** and ethanolamine (10 mmol). The compound was obtained in a 45 % yield, R_f = 0.57 in EA:CH_2Cl_2 (2:3), Mp 185–187 °C. ^{1}H NMR (400 MHz, DMSO-d_6): δ (ppm) 3.66–3.70 (4H, m), 4.85 (1H, s), 6.95 (1H, d, $J = 4.4$ Hz), 7.37 (1H, td, $J = 8.4$, 1.2 Hz), 7.60 (1H, t, $J = 8.4$ Hz), 7.69 (2H, t, $J = 6$ Hz), 7.84 (1H, t, $J = 8.4$ Hz), 7.94 (1H, d, $J = 8$ Hz), 8.46 (1H, d, $J = 8$ Hz), 9.35 (1H, d, $J = 8$ Hz). ^{13}C NMR (100 MHz, DMSO-d_6): δ (ppm) 44.76, 59.84, 120.46, 124.08, 125.19, 125.93, 127.01, 127.12, 128.46, 129.32, 129.45, 129.65, 131.08, 133.32, 133.51, 145.54, 151.61, 181.89. HRMS (ESI) *m/z* calcd. for $C_{18}H_{13}N_2O_2S^+$ [M]$^+$: 321.0692; found [M + H]$^+$: 323.0851.

2.1.1.3.12. 6-(3-hydroxypropylamino)-12H-thiochromeno[2, 3-c]quinolin-12-one (14). Compound **14** was prepared from **4** and 3-amino-1-propanol (6 mmol). The compound was obtained in a 91 % yield, R_f = 0.57 in EA:CH_2Cl_2 (2:3), Mp 166–168 °C. ^{1}H NMR (400 MHz, DMSO-d_6): δ (ppm) 1.87 (2H, quin, $J = 6.4$ Hz), 3.58 (2H, q, $J = 5.6$ Hz), 3.64 (2H, q, $J = 6.4$ Hz), 4.69 (1H, t, $J = 5.2$ Hz), 7.07 (1H, t, $J = 5.2$ Hz), 7.33 (1H, t, $J = 8.4$ Hz), 7.56 (1H, td, $J = 8$, 1.2 Hz), 7.64 (1H, t, $J = 8$ Hz), 7.78 (1H, td, $J = 8$, 1.2 Hz), 7.88 (1H, d, $J = 7.6$ Hz), 8.42 (1H, dd, $J = 8$, 0.8 Hz), 9.33 (1H, dd, $J = 8.8$, 0.8 Hz). ^{13}C NMR (100 MHz, DMSO-d_6): δ (ppm) 31.63, 59.20, 119.90, 123.44, 124.74, 125.46, 126.49, 126.54, 127.87, 128.71, 128.92, 129.06, 130.55, 132.73, 133.06, 145.13, 151.09, 181.34. HRMS (ESI) *m/z* calcd. for $C_{19}H_{15}N_2O_2S^+$ [M]$^+$: 335.0849; found [M + H]$^+$: 337.1005.

2.1.1.3.13. 6-(5-hydroxypentylamino)-12H-thiochromeno[2, 3-c]quinolin-12-one (15). Compound **15** was prepared from **4** and 5-amino-1-pentanol (3 mmol). The compound was obtained in a 71 % yield, R_f = 0.53 in EA:CH_2Cl_2 (2:3), Mp 139–141 °C. ^{1}H NMR (400 MHz, DMSO-d_6): δ (ppm) 1.37–1.44 (2H, m), 1.47–1.54 (2H, m), 1.71 (2H, quin, $J = 7.2$ Hz), 3.42 (2H, q, $J = 6$ Hz), 3.57 (2H, q, $J = 6.4$ Hz), 4.36 (1H, t, $J = 5.2$ Hz), 7.07 (1H, t, $J = 5.2$ Hz), 7.34 (1H, td, $J = 8.4$ Hz, 1.6 Hz), 7.57 (1H, td, $J = 8.8$, 1.6 Hz), 7.64–7.69 (2H, m), 7.81 (1H, t, $J = 8.4$ Hz), 7.90 (1H, d, $J = 8$ Hz), 8.44 (1H, dd, $J = 8$, 1.2 Hz), 9.34 (1H, dd, $J = 8.4$, 1.2 Hz). ^{13}C NMR (100 MHz, DMSO-d_6): δ (ppm) 23.66, 28.88, 32.83, 42.10, 61.20, 120.35, 123.86, 125.26, 125.91, 127.06, 128.37, 129.20, 129.41, 129.53, 131.05, 133.24, 133.63, 145.70, 151.53, 181.88. HRMS (ESI) *m/z* calcd. for $C_{21}H_{19}N_2O_2S^+$ [M]$^+$: 363.1162; found [M + H]$^+$: 365.1324.

2.1.1.3.14. 6-(2-methoxyethylamino)-12H-thiochromeno[2, 3-c]quinolin-12-one (16). Compound **16** was prepared from **4** and 2-methoxyethylamine (3 mmol). The compound was obtained in a 69 % yield, R_f = 0.9 in EA:CH_2Cl_2 (2:3), Mp 133–135 °C. ^{1}H NMR (400 MHz, DMSO-d_6): δ (ppm) 3.46 (3H, s), 3.72 (2H, t, $J = 5.2$ Hz), 3.88 (2H, q, $J = 5.2$ Hz), 5.34 (2H, t, $J = 4.8$ Hz), 7.40 (1H, t, $J = 8$ Hz), 7.37–7.59 (4H, m), 7.76 (1H, d, $J = 8.4$ Hz), 8.48 (1H, d, $J = 8$ Hz), 9.42 (1H, dd, $J = 8.8$ Hz).). ^{13}C NMR (100 MHz, DMSO-d_6): δ (ppm) 41.75, 58.84, 70.89, 120.86, 124.00, 124.30, 125.82, 125.89, 126.92, 127.37, 129.05, 129.46, 129.71, 131.29, 131.87, 132.77, 145.28, 150.59, 181.89. HRMS (ESI) *m/z* calcd. for $C_{19}H_{15}N_2O_2S^+$ [M]$^+$: 335.0849; found [M + H]$^+$: 337.1011.

2.1.1.3.15. 6-(2-(Methylamino)ethylamino)-12H-thiochromeno[2, 3-c]quinolin-12-one (17). Compound **17** was prepared from **4** and N-methyl ethylenediamine (6 mmol). The compound was obtained in a 47 % yield. R_f = 0.47 in MeOH: CH_2Cl_2 (1:4), Mp 155–157 °C. ^{1}H NMR (400 MHz, DMSO-d_6): δ (ppm) 2.54 (3H, s), 3.01 (2H, t, $J = 6$ Hz), 3.80 (2H, s), 5.72 (1H, s), 7.43 (1H, t, J = 8.4), 7.57–7.67 (4H, m), 7.81 (1H, dd, $J = 8.4$, 0.8 Hz), 8.58 (1H, d, $J = 8$ Hz), 9.47 (1H, dd, $J = 8.4$, 0.8 Hz). ^{13}C NMR (100 MHz, DMSO-d_6): δ (ppm) 36.13, 41.26, 50.37, 120.89, 124.21, 124.33, 125.96, 126.03, 126.97, 127.53, 129.21, 129.70, 129.92, 131.59, 132.04, 133.09, 145.57, 151.02, 182.20. HRMS (ESI) *m/z* calcd. for $C_{19}H_{16}N_3OS^+$ [M]$^+$: 334.1009; found [M + H]$^+$: 336.1172.

2.1.1.3.16. 6-(2-(Dimethylamino)ethylamino)-12H-thiochromeno[2, 3-c]quinolin-12-one (18). Compound **18** was prepared from **4** and N, N-dimethylethylenediamine (4.5 mmol). The compound was obtained in a 52 % yield. R_f = 0.67 in MeOH: CH_2Cl_2 (1:4), Mp 157–159 °C. ^{1}H NMR (400 MHz, DMSO-d_6): δ (ppm) 2.36 (6H, s), 2.69 (2H, t, $J = 6.0$ Hz), 3.75 (2H, q, $J = 5.2$ Hz), 5.85 (1H, s), 7.42 (1H, t, J = 7.2), 7.55–7.70 (4H, m), 7.81 (1H, d, $J = 8.4$ Hz), 8.58 (1H, d, $J = 8$ Hz), 9.48 (1H, d, $J = 8.8$ Hz). ^{13}C NMR (100 MHz, DMSO-d_6): δ (ppm) 39.53, 45.30, 57.62, 120.84, 124.24, 124.32, 125.96, 126.04, 126.92, 127.49, 129.18, 129.68, 129.83, 131.59, 132.00, 133.0, 145.63, 151.01, 182.21. HRMS (ESI) *m/z* calcd. for $C_{20}H_{18}N_3OS^+$ [M]$^+$: 348.1165; found [M + H]$^+$: 350.1328.

2.1.1.3.17. 6-(2-(2-hydroxyethylamino)ethylamino)-12H-thiochromeno[2,3-c]quinolin-12-one (19). Compound **19** was prepared from

4 and N-(2-hydroxyethyl)ethylenediamine (4.9 mmol). The compound was obtained in a 49 % yield. R_f = 0.43 in MeOH:CH_2Cl_2 (1:4), Mp 158–160 °C. ^{1}H NMR (400 MHz, DMSO-d_6): δ (ppm) 2.15 (1H), 2.66 (2H, t, J = 6 Hz), 2.89 (2H, t, J = 6.4 Hz), 3.48 (2H, s), 3.66 (2H, t, J = 6.4 Hz), 4.49 (1H, s), 7.01 (1H, s), 7.37 (1H, t, J = 8.4 Hz), 7.59 (1H, td, J = 8.4, 1.2 Hz), 7.67–7.71 (2H, m), 7.84 (1H, t, J = 8.4 Hz), 7.95 (1H, d, J = 8 Hz), 8.46 (1H, dd, J = 8 Hz, 0.8 Hz), 9.36 (1H, d, J = 8.4 Hz). ^{13}C NMR (100 MHz, DMSO-d_6): δ (ppm) 42.06, 48.27, 51.85, 60.94, 120.40, 124.01, 125.20, 125.89, 127.04127.10, 128.42, 129.23, 129.41, 129.58, 131.04, 133.27, 133.49, 145.59, 151.56, 181.86. HRMS (ESI) *m/z* calcd. for $C_{20}H_{18}N_3O_2S^+$ $[M]^+$: 364.1114; found $[M + H]^+$: 366.1274.

2.1.1.3.18. 6-(3-(2-hydroxyethylamino)propylamino)-12H-thiochromeno[2,3-c]quinolin-12-one (20). Compound **20** was prepared from **4** and N-(2-hydroxyethyl)ethylenediamine (4.2 mmol). The compound was obtained with an 84 % yield. R_f = 0.25 in MeOH:AcOH (9:1), Mp 149–151 °C. ^{1}H NMR (400 MHz, DMSO-d_6): δ (ppm) 1.84 (2H, quin, J = 6 Hz), 2.65 (2H, t, J = 6 Hz), 2.73 (2H, t, J = 6.4 Hz), 3.57 (2H, t, J = 5.6 Hz), 3.64 (2H, t, J = 6.4 Hz), 4.58 (1H, s), 7.35 (1H, t, J = 8 Hz), 7.57 (1H, t, J = 7.6 Hz, Ar-H9), 67–7.69 (2H, m, Ar-H3,10), 7.83 (1H, t, J = 7.6 Hz, Ar-H8), 7.88 (1H, d, J = 8 Hz, Ar-H1), 8.45 (1H, d, J = 8 Hz, Ar-*H*11), 9.35 (1H, d, J = 8.4 Hz). ^{13}C NMR (100 MHz, DMSO-d_6): δ (ppm) 28.40, 41.98, 48.56, 52.28, 60.89, 120.31, 123.82, 125.31, 125.93, 127.02, 128.39, 129.13, 129.44, 129.53, 131.06, 133.26, 133.60, 145.78, 151.56, 181.87. HRMS (ESI) *m/z* calcd. for $C_{21}H_{20}N_3O_2S^+$ $[M]^+$: 378.1271; found $[M + H]^+$: 380.1431.

2.1.1.3.19. 6-(Cyclopropylmethylamino)-12H-thiochromeno[2, 3-c]quinolin-12-one (21). Compound **21** was prepared from **4** and cyclopropanemethylamine (7 mmol). The compound was obtained in a 56 % yield. R_f = 0.77 in CH_2Cl_2, Mp = 169–171 °C. 1H NMR (400 MHz, CDCl3): δ (ppm) 0.39 (2H, q, J = 4.8 Hz, –CH2-), 0.62–0.66 (2H, m, –CH2-), 1.23–1.29 (1H, m, –CH-), 3.56 (2H, q, J = 5.2 Hz, –CH2-), 5.02 (1H, t, J = 4.8 Hz, –NH-), 7.41–7.45 (1H, m, Ar-H2), 7.55–7.66 (4H, m, Ar-H3,8,9,10), 7.80 (1H, dd, J = 8.4, 0.8 Hz, Ar-H1), 8.57 (1H, d, J = 8 Hz, Ar-*H*11), 9.46 (1H, dd, J = 8.4, 0.8 Hz, Ar-H4). 13C NMR (100 MHz, CDCl3): δ (ppm) 3.65, 10.73, 47.49, 120.86, 123.73, 124.36, 125.92, 125.96, 127.02, 127.56, 129.22, 129.71, 129.94, 131.57, 132.07, 132.89, 145.55, 150.71, 182.16. HRMS (ESI) *m/z* calcd. for $C_{20}H_{15}N_2OS^+$ $[M]^+$: 331.0900; found $[M + H]^+$: 333.1057.

2.1.1.3.20. 6-(Cyclopentylamino)-12H-thiochromeno[2, 3-c]quinolin-12-one (22). Compound **22** was prepared from **4** and cyclopentylamine (5 mmol). The compound was obtained in a 50 % yield. R_f = 0.8 in CH_2Cl_2, Mp = 153–155 °C. ^{1}H NMR (400 MHz, $CDCl_3$): δ (ppm) 1.59–1.64 (2H, m, –CH_2-), 1.69–1.86 (4H, m, –CH_2-), 2.27 (2H, J = 6 Hz, –CH_2-), 4.66 (1H, J = 6.4 Hz, –CH-), 4.87 (1H, d, J = 6 Hz, –NH-), 7.42 (1H, t, J = 8.4 Hz, Ar-H_2), 7.54–7.65 (4H, m, Ar-$H_{3,8,9,10}$), 7.82 (1H, dd, J = 8.4, 0.8 Hz, Ar-H_1), 8.56 (1H, d, J = 7.6 Hz, Ar-H_{11}), 9.46 (1H, dd, J = 8.4, 0.8 Hz, Ar-H_4). ^{13}C NMR (100 MHz, $CDCl_3$): δ (ppm) 24.03, 33.53, 53.82, 120.76, 123.75, 124.27, 125.89, 125.95, 127.21, 127.56, 129.17, 129.74, 129.94, 131.62, 132.07, 132.90, 145.71, 15.51, 182.23. HRMS (ESI) *m/z* calcd. for $C_{21}H_{17}N_2OS^+$ $[M]^+$: 345.1056; found $[M + H]^+$: 347.1223.

2.1.1.3.21. 6-(Cyclohexylamino)-12H-thiochromeno[2, 3-c]quinolin-12-one (23). Compound **23** was prepared from **4** and cyclohexylamine (4 mmol). The compound was obtained in a 57 % yield. R_f = 0.83 in CH_2Cl_2, Mp = 128–130 °C. ^{1}H NMR (400 MHz, $CDCl_3$): δ (ppm) 1.15–1.24 (1H, m, –CH_2-), 1.35–1.53 (4H, sep, J = 11.6 Hz, –CH_2-), 1.65 (2H, quin, J = 13.2 Hz, –CH_2-), 1.78 (2H, q, J = 12.8 Hz, –CH_2-), 2.02 (2H, q, J = 11.2 Hz, –CH_2-), 4.18–4.26 (1H, m, –CH-), 6.57 (1H, d, J = 7.6 Hz, –NH-), 7.35 (1H, td, J = 9.2, 1.2 Hz, Ar-H_2), 7.58 (1H, t, J = 8.8 Hz, Ar-H_9), 7.68 (2H, t, J = 8 Hz, Ar-$H_{3,10}$), 7.83 (1H, t, J = 8 Hz, Ar-H_8), 7.93 (1H, d, J = 8 Hz, Ar-H_1), 8.45 (1H, d, J = 8 Hz, Ar-H_{11}), 9.34 (1H, d, J = 8.4 Hz, Ar-H_4). ^{13}C NMR (100 MHz, $CDCl_3$): δ (ppm) 25.58, 25.99, 32.45, 50.72, 120.38, 123.98, 125.36, 125.86, 127.05, 127.10, 128.39, 129.35, 129.41, 129.57, 131.03, 133.28, 133.72, 145.61, 150.86, 181.93. HRMS (ESI) *m/z* calcd. for $C_{22}H_{19}N_2OS^+$ $[M]^+$: 359.1213; found $[M + H]^+$: 361.1375.

2.1.1.3.22. 6-(2-morpholinoethylamino)-12H-thiochromeno[2, 3-c]quinolin-12-one (24). Compound **24** was prepared from **4** and 4-(2-aminoethyl)morpholine (4 mmol). The compound was obtained in a 49 % yield. R_f = 0.27 in EA:CH_2Cl_2 (2:3), Mp = 136–138 °C. ^{1}H NMR (400 MHz, $CDCl_3$): δ (ppm) 2.60 (4H, t, J = 4.4 Hz, –CH2-), 2.79 (2H, t, J = 6 Hz, –CH2-), 3.77–3.82 (6H, m, –CH2-), 5.91 (1H, s, –NH-), 7.44 (1H, t, J = 8.4 Hz, Ar-H2), 7.58–7.63 (2H, m, Ar-H9,10), 7.67–7.73 (2H, m, Ar-H3,8), 7.81 (1H, d, J = 8 Hz, Ar-H1), 8.60 (1H, d, J = 8.4 Hz, Ar-*H*11), 9.48 (1H, dd, J = 8.4, 1.6 Hz, Ar-H4). ^{13}C NMR (100 MHz, $CDCl_3$): δ (ppm) 38.30, 53.29, 56.47, 67.25, 120.88, 124.10, 124.35, 125.97, 126.06, 126.94, 127.58, 129.24, 129.73, 129.94, 131.62, 132.07, 133.03, 145.62, 150.90, 182.16. HRMS (ESI) *m/z* calcd. for $C_{22}H_{20}N_3O_2S^+$ $[M]^+$: 390.1271; found $[M + H]^+$: 392.1426.

2.1.1.3.23. 6-(Dimethylamino)-12H-thiochromeno[2, 3-c]quinolin-12-one (25). Compound **25** was prepared from **4** and dimethylamine (4.5 mmol). The compound was obtained in a 96 % yield. R_f = 0.87 in CH_2Cl_2, Mp = 141–142 °C. ^{1}H NMR (400 MHz, $CDCl_3$): δ (ppm) 3.07 (6H, s, –CH3), 7.54–7.70 (5H, m, Ar-H2,3,8,9,10), 7.98 (1H, dd, J = 8.4, 1.2 Hz, Ar-H1), 8.59 (1H, dt, J = 8.4, 0.8 Hz, Ar-*H*11), 9.61 (1H, dd, J = 8.4, 1.2 Hz, Ar-H4). ^{13}C NMR (100 MHz, $CDCl_3$): δ (ppm) 42.96, 123.52, 125.74, 126.18, 126.96, 127.13, 128.37, 129.13, 129.44, 130.56, 130.96, 131.25, 132.03, 136.02, 144.75, 158.34, 182.68. HRMS (ESI) *m/z* calcd. for $C_{18}H_{13}N_2OS^+$ $[M]^+$: 305.0743; found $[M + H]^+$: 307.0903.

2.1.1.3.24. 6-(((1,3-dioxolan-2-yl)methyl)(methyl)amino)-12H-thiochromeno[2, 3-c]quinolin-12-one (26). Compound **26** was prepared from **4** and 2-methylaminomethyl-1,3-dioxolane (4.4. mmol). The compound was obtained in a 51 % yield. R_f = 0.57 in CH_2Cl_2, Mp = 127–128 °C. ^{1}H NMR (400 MHz, $CDCl_3$): δ (ppm) 3.13 (3H, s, –CH3), 3.65 (2H, d, J = 4.4 Hz, –CH2-), 3.82–3.90 (2H, m, –CH2-), 3.94–4.00 (2H, m, –CH2-), 5.26 (1H, q, J = 4.4 Hz, –CH-), 7.50 (1H, t, J = 8 Hz, Ar-H2), 7.56–7.68 (4H, m, Ar-H3,8,9,10), 7.96 (1H, dd, J = 8, 0.8 Hz, Ar-H1), 8.54 (1H, dd, J = 8, 0.8 Hz, Ar-*H*11), 9.60 (1H, dd, J = 8.8, 0.8 Hz, Ar-H4). ^{13}C NMR (100 MHz, $CDCl_3$): δ (ppm) 42.26, 56.84, 64.87, 103.14, 123.65, 125.68, 126.17, 126.99, 127.14, 128.37, 128.98, 129.26, 130.91, 131.03, 131.87, 135.91, 144.46, 157.87, 182.418. HRMS (ESI) *m/z* calcd. for $C_{21}H_{17}N_2O_3S^+$ $[M]^+$: 377.0954; found $[M + H]^+$: 379.1114.

2.1.1.3.25. 6-(Piperidin-1-yl)-12H-thiochromeno[2, 3-c]quinolin-12-one (27). Compound **27** was prepared from **4** and piperidine (5 mmol). The compound was obtained in a 69 % yield. R_f = 0.93 in CH_2Cl_2, Mp = 168–169 °C. ^{1}H NMR (400 MHz, $CDCl_3$): δ (ppm) 1.72 (2H, d, J = 4.8 Hz, –CH2-), 1.88 (4H, t, J = 5.2 Hz, –CH2-), 3.33 (4H, s, –CH2-), 7.53–7.71 (5H, m, Ar-H2,3,8,9,10), 7.98 (1H, d, J = 8 Hz, Ar-H1), 8.59 (1H, d, J = 8 Hz, Ar-*H*11), 9.63 (1H, d, J = 8.4 Hz, Ar-H4). ^{13}C NMR (100 MHz, $CDCl_3$): δ (ppm) 24.32, 25.91, 52.29, 123.58, 125.81, 126.27, 127.01, 127.03, 128.47, 128.99, 129.42, 130.81, 131.20, 131.63, 131.92, 136.35, 144.90, 158.55, 182.69. HRMS (ESI) *m/z* calcd. for $C_{21}H_{17}N_2OS^+$ $[M]^+$: 345.1056; found $[M + H]^+$: 347.1218.

2.1.1.3.26. 6-(4-hydroxypiperidin-1-yl)-12H-thiochromeno[2, 3-c]quinolin-12-one (28). Compound **28** was prepared from **4** and 4-hydroxypiperidine (3 mmol). The compound was obtained in a 29 % yield. R_f = 0.57 in EA:CH_2Cl_2 (2:3), Mp = 209–210 °C. ^{1}H NMR (400 MHz, $CDCl_3$): δ (ppm) 1.64 (1H, s, –OH), 1.89–1.98 (2H, m, –CH2-), 2.16–2.20 (2H, m, –CH2-), 3.19 (2H, t, J = 12.8 Hz, –CH2-), 3.63–3.68 (2H, m, –CH2-), 4.01 (1H, sep, J = 4.4 Hz, –CH-), 7.55–7.72 (5H, m, Ar-H2,3,8,9,10), 7.98 (1H, d, J = 8 Hz, Ar-H1), 8.60 (1H, d, J = 8.8 Hz, Ar-*H*11), 9.64 (1H, d, J = 8.8 Hz, Ar-H4). ^{13}C NMR (100 MHz, $CDCl_3$): δ (ppm) 34.52, 48.87, 67.90, 123.73, 125.88, 126.32, 127.17, 127.30, 128.55, 129.13, 129.52, 130.96, 131.26, 131.32, 132.08, 136.14, 144.84, 157.89, 182.67. HRMS (ESI) *m/z* calcd. for $C_{21}H_{17}N_2O_2S^+$ $[M]^+$: 361.1005; found $[M + H]^+$: 363.1163.

2.1.1.3.27. 6-(1,4′-bipiperidin-1′-yl)-12H-thiochromeno[2, 3-c]quinolin-12-one (29). Compound **29** was prepared from **4** and 4-piperidinopiperidine (2.5 mmol). The compound was obtained in a 38 % yield. R_f = 0.7 in MeOH:CH_2Cl_2 (1:4), Mp = 185–187 °C. ^{1}H NMR (400 MHz,

$CDCl_3$): δ (ppm) 1.50–1.53 (2H, m, –CH2-), 1.66 (4H, quin, $J = 5.6$ Hz, –CH2-), 1.78 (2H, s, –CH2-), 1.93 (2H, qd, $J = 13.6$, 4 Hz, –CH2-), 2.06 (2H, d, $J = 10.8$ Hz, –CH2-), 2.48–2.56 (1H, m, –CH-), 2.61–2.66 (4H, m, –CH2-), 3.04 (2H, t, $J = 11.2$ Hz, –CH2-), 3.76 (2H, d, $J = 12.8$ Hz, –CH2-), 7.55–7.71 (5H, m, Ar-H2,3,8,9,10), 7.98 (1H, dd, $J = 8.4$, 0.8 Hz, Ar-H1), 8.60 (1H, d, $J = 8.4$ Hz, Ar-*H*11), 9.64 (1H, dd, $J = 8.4$, 1.2 Hz, Ar-H4). ^{13}C NMR (100 MHz, $CDCl_3$): δ (ppm) 24.83, 26.43, 28.28, 50.47, 51.13, 62.45, 123.67, 125.85, 126.29, 127.10, 127.17, 128.51, 129.07, 129.48, 130.86, 131.23, 131.45, 132.02, 136.25, 144.86, 158.00, 182.67. HRMS (ESI) *m/z* calcd. for $C_{26}H_{26}N_3OS^+$ $[M]^+$: 428.1791; found $[M + H]^+$: 430.1946.

2.1.1.3.28. 6-(1,4-dioxa-8-azaspiro[4.5]decan-8-yl)-12H-thiochromeno[2,3-c]quinolin-12-one (30). Compound **30** was prepared from **4** and 4-piperidone-ethylene ketal (4 mmol). The compound was obtained in a 40 % yield. $R_f = 0.83$ in EA:CH_2Cl_2 (2:3), Mp = 201–203 °C. ^{1}H NMR (400 MHz, $CDCl_3$): δ (ppm) 2.05 (4H,t, $J = 5.6$ Hz, –CH2-), 3.50 (4H,t, $J = 5.6$ Hz, –CH2-), 4.05 (4H,s, –CH2-), 7.55–7.72 (5H, m, Ar-H2,3,8,9,10), 7.98 (1H, dd, $J = 8$,1.2 Hz, Ar-H1), 8.60 (1H, dd, $J = 8$, 0.8 Hz, Ar-*H*11), 9.64 (1H, dd, $J = 8.4$, 1.2 Hz, Ar-H4). ^{13}C NMR (100 MHz, $CDCl_3$): δ (ppm) 35.06, 49.26, 64.44, 107.11, 123.66, 125.82, 126.30, 127.14, 127.22, 128.62, 129.09, 129.49, 130.90, 131.12, 131.24, 132.04, 136.10, 144.84, 157.63, 182.67. HRMS (ESI) *m/z* calcd. for $C_{23}H_{19}N_2O_3S^+$ $[M]^+$: 403.1111; found $[M + H]^+ = 405.1277$.

2.2. Biological evaluation

2.2.1. Initial in vitro cytotoxicity screening of compounds

To investigate the potential cytotoxic effects of synthesized compounds **5** ∼ **30**, MTT assays were performed to determine the 50 % inhibitory concentration (IC_{50}) values of each compound against the MCF-7 and MDA-MB-468 human breast carcinoma cell lines. These cell lines were obtained from American Type Culture Collection (USA) and cultured in Dulbecco's modified Eagle's medium (DMEM) supplemented with 10 % heat-inactivated fetal bovine serum (FBS) at 37 °C in a humidified atmosphere containing 5 % CO_2 co.

MCF-7 and MDA-MB-468 cells were seeded (at 3000 cells/well) in 96-well microplates containing DMEM supplemented with 10 % FBS and treated with various concentrations of the compounds for 72 h. The microplates were rinsed three times with phosphate-buffered saline (PBS) after treatment, and 100 μL of an MTT solution (at a final concentration of 0.5 mg/mL in the medium) was added to each well, followed by incubation at 37 °C for 1 h. Mitochondrial succinate dehydrogenase was used to convert MTT to blue formazan crystals. The microplates were washed again with PBS and then solubilized with 100 μL of DMSO per well. The absorbance at 540 nm was measured using an enzyme-linked immunosorbent assay (ELISA) microplate reader to determine the effects of the synthetic compounds on cell viability as relative activities.

2.2.2. One-dose and five-dose assays of the NCI-60 human tumor cell lines screening program

We conducted experiments to test the growth-inhibition capabilities of our selected compounds against a panel of 60 human cancer cell lines under the NCI drug screening program. Initially, the compounds were tested at a single high dose concentration of 10 μM. Subsequently, those compounds that demonstrated significant growth-inhibitory capabilities and fulfilled the predetermined threshold inhibition criteria of the NCI were selected to proceed to the five-dose assay. The methodology used in this study was described in detail in our previous publications (Chen et al., 2019; Chen et al., 2019).

2.3. In silico study

2.3.1. Drug-likeness, ADME, and toxicity predictions

The drug-likeness, ADME (Absorption, Distribution, Metabolism, and Excretion), and toxicity properties of all synthesized compounds were predicted using the online software tools swissADME (http://www.swissadme.ch/) (Daina et al., 2017; Daina et al., 2014) and ADMETlab 2.0 (https://admetmesh.scbdd.com/) (Xiong et al., 2021; Dong et al., 2018).

2.3.2. Identification of drugs with similar profiles to our compounds by a COMPARE analysis

Results from the NCI five-dose cytotoxicity studies of compounds **18** (NSC784447) and **20** (NSC784449) were used as a "seed" in COMPARE algorithms to correlate with investigational drugs and standard drugs in NCI databases using Pearson's correlation coefficient calculations. At the same time, GI_{50}, TGI, and LC_{50} were set as endpoints (Ali et al., 2016; Lawal et al., 2021).

2.3.3. Molecular modeling

Crystal structures of recombinant human topoisomerase (TOPO) I (PDB ID: 1EJ9) (Redinbo et al., 2000), TOPO II (PDB ID: 4FM9) (Wendorff et al., 2012), CDK4 (PDB ID: 2W9Z) (Day et al., 2009), AURKA (PDB ID: 5ORY) (McIntyre et al., 2017), and CDK6 (PDB ID: 3NUP) (Cho et al., 2010) were downloaded from the protein data bank (PDB) site (https://www.rcsb.org/). Pymol was used to prepare protein structures (Schrödinger and DeLano, 2020). Avogadro optimized the ligand structure, bond length, and bond angle after the 2D ligand structure was created with ChemDraw Ultra 12.0 software (Hanwell et al., 2012). The ligand and protein receptor were both saved as PDB files.

Auto dock vina software (Eberhardt et al., 2021; Trott and Olson, 2010) was used for docking investigations after the above procedures were finished. Auto-dock was used to import the prepared PDB files (proteins and ligands) and save them in pdbqt file format. Further, amino acids from the active sites were also targeted to correct the grid parameters. The Discovery Studio Visualizer 2021 client was used to examine and visualize these docking conformations (in both 2D and 3D).

3. Result and discussion

3.1. Chemistry

Compound **3** was sequentially synthesized by the Pfitzinger reaction using isatin and (thiophenyl) acetic under alkaline conditions. The acid reaction resulted in 2-hydroxy-3-(phenylthio) quinoline-4-carboxylic acid (1). This is because the amide bond is easily hydrolyzed in alkaline conditions, opening the ring and forming ketoacids. When the loop is opened, the intermediate is easily converted to quinoline-4-carboxylic acid compounds by reacting with (thiophenyl) acetic acid (carbonyl compound) (Komatsu et al., 2023). Chlorination and a cyclization reaction were used to obtain 6-chloro-12H-thiochromeno [2,3–c] quinoline-12-one (compound **4**) using $POCl_3$. The synthesis of **5**–**30** was carried out via amination of **4** with various suitable primary amines, secondary amines, and sodium bicarbonate. The appropriate primary and secondary amines and **4** were reacted in DMSO to form **5**–**30** (35 %–96 %), respectively. The detailed reaction process is shown in Scheme 2. ^{1}H nuclear magnetic resonance (NMR), ^{13}C NMR, and high-resolution mass spectroscopy (HRMS) spectra were used to determine their chemical compositions.

Compound **3** structurally contains an acid group (–COOH) according to ^{1}H NMR results, where a peak was found at 11–13 ppm, and according to ^{13}C NMR results, where the acid group (–COOH) was located at 166.44 ppm. However, the carbonyl group (C = O) of compound **4** in the ^{13}C NMR signal was found at 181.52 ppm, demonstrating the peak that resulted from the substitution of a carbonyl group (C = O) for an acid group (–COOH) on the structure. The sixth position of compounds **4**, **5**, and **25** were utilized based on ^{13}C NMR results. After additional functional groups replaced the position of chlorine in the primary structure, the direction of the low magnetic field chemically shifted due to carbon atoms (downfield). When the substituted group was a primary amine (compound **5**), the peak showed its location in both ^{1}H NMR and ^{13}C

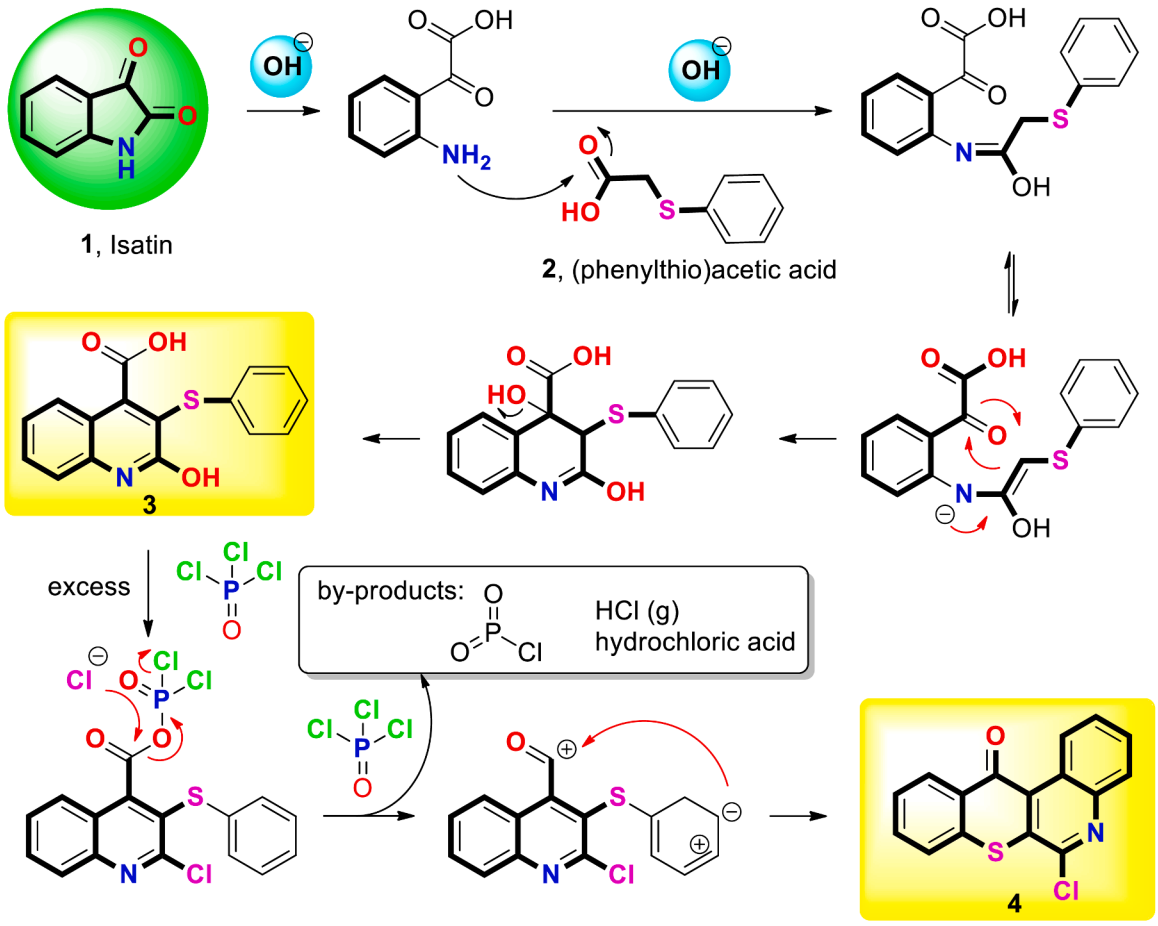

Scheme 2. Mechanism and plausible catalytic cycle during Pfitzinger reaction and cyclization.

NMR results, and the corresponding position was demonstrated to be a substitution of secondary amines (compound **25**) biased toward a strong magnetic field (upfield) (Table S1).

The conditions, times, and yields of reactions differed depending on the amine type. The reaction yield could be decreased, and in some cases, the reaction proceeded only under controlled temperature conditions. Therefore, in these kinds of processes, temperature control is essential (Table S4). Furthermore, due to limited yield, it was challenging to obtain crystalline material for the most promising compounds, specifically compounds 18 and 20. However, compound 25 yielded large crystals when crystallized in hot CH_2Cl_2 with a slow evaporation process, allowing its structural determination by SC-XRD (Fig. 2, Table S2).

3.2. Biological evaluation

3.2.1. In vitro cytotoxicity screening of compounds and structure–activity relationship (SAR) studies

We tested the toxicity of active substances against MCF-7 and MDA-MB-468 human breast cancer cells. SAR data revealed that most of the compounds had potent cytotoxic effects and that primary amine substitutions (IC_{50} values of 2.3 to > 20 mM) had stronger anticancer activity than secondary or tertiary amine substitutions. Additionally, an alkylamine substitution showed that the carbon side chain length of the 6H-thiochromeno [2,3-c] quinoline-12 (12H)-one scaffold was essential for enhancing the cytotoxic effects of our synthesized compounds.

Compounds **5**, **17**, **18**, **19**, **20**, and **24** exhibited the lowest IC_{50} values against MCF7 and MDA-MB-468 cells out of all the synthesized compounds (Table 1). However, antiproliferative results for compounds **9**, **10**, **15**, and **23** only demonstrated anticancer activities in MDA-MB-468 cells, while compound **21** only demonstrated such activities in MCF-7 cells (other compounds showed IC_{50} values of > 20 μM in both cell lines).

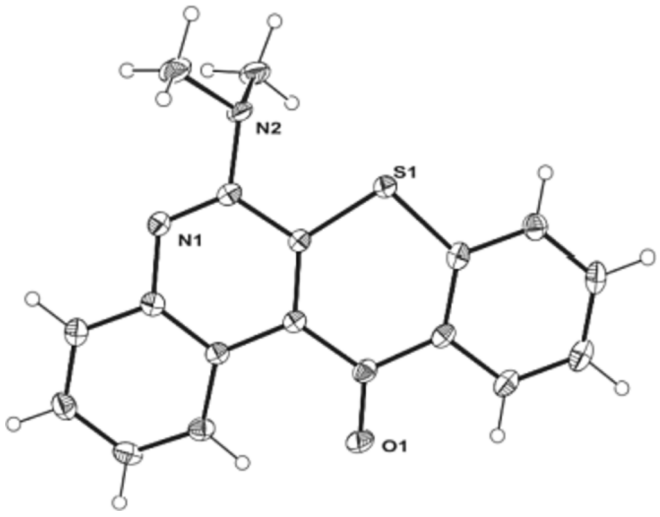

Fig. 2. ORTEP diagram of compound **25.**

As shown in Table 2, we further investigated the selectivity index (SI) to analyze the sensitivities of compounds **5**, **17**, **18**, **19**, **20**, and **24** against both MCF7 and MDA-MB-468 cells. Compounds **5**, **17**, **18**, **19**, and **20** exhibited high sensitivity (SI > 1) toward MCF-7 cells, while only compounds **5** and **17** showed high sensitivity toward MDA-MB-468

cells. Compounds **18, 19,** and **20** displayed no sensitivity (SI < 1) toward MDA-MB-468 cells. However, compound **24** showed no selectivity (SI < 1) toward either cell line. Overall, compounds **17** and **18** were the most active and sensitive among these TC-S-1 derivatives against both MCF7 and MDA-MB-468 cells.

3.2.2. *Evaluation of the cytotoxic activities of compounds by one-dose assays of the NCI-60 human tumor cell line screening program*

Nine compounds, including **6** (NSC784437), **7** (NSC784438), **16** (NSC784445), **18** (NSC784447), **20** (NSC784449), **24** (NSC784440), **25** (NSC784442), **28** (NSC784441), and **30** (NSC784444), were selected by the one-dose assays of the NCI to be evaluated against various types of cancer, including leukemia, non-small cell lung cancer (NSCLC), colon cancer, central nervous system (CNS) cancers, melanomas, ovarian cancers, renal cancers, prostate cancer, and breast cancer (Martorana et al., 2022). We primarily evaluated these nine compounds for their antiproliferative and cytotoxic effects against the NCI-60 cell lines. The results of each drug were expressed as the ratio of the growth percentage of cells treated with a compound concentration at 10 μM to the growth percentage of untreated control cells. Among the evaluated compounds, **18** (NSC784447) and **20** (NSC784449) demonstrated anticancer activities against these cancer cell lines.

The most inhibited cell lines after treatment with compound **18** (NSC784447) were LOX IMVI, COLO 205, M14, SK-MEL-5, MCF7, SW-620, MDA-MB-468, and K-562 which showed respective growth percentages of −91.59 %, −9.58 %, −54.67 %, −83.13 %, −46.92 %, −54.03 %, –23.62 %, and −35.06 %. For **20** (NSC784449), the most affected cell lines were MCF7, MDA-MB-468, COLO 205, SW-620, LOX IMVI, M14, SK-MEL-5 and HCT-116 which showed respective growth percentages of −72.93 %, −57.26 %, −78.95 %, −62.45 %, −87.42 %, −61.84 %, 64.67 %, and −57.48 % (Fig. 3). Compound **24** (NSC784440) showed inhibitory effects against the K-562 and SF295 cell lines and reduced their growth percentages to −11.67 % and −7.24 %.

Multiple cancer cell lines responded effectively to the initial single doses of **18** (NSC784447) and **20** (NSC784449) of 10 μM, indicating the need for further research into the dose-dependent effects. However, for this investigation, we primarily focused on data related to breast cancer.

3.2.3. *Compounds 18 (NSC784447) and 20 (NSC784449) exhibit dose-dependent anticancer activities tested by five-dose assays of NCI-60 human cancer cell*

Further investigation was carried out since NCI-60 one-dose screening parameters for threshold inhibition were met by **18** (NSC784447) and **20** (NSC784449) in equal measure. Five dosages of our compounds were evaluated in each cell line. Compound **18** (NSC784447) and **20** (NSC784449) dose–response curves were plotted using the percentages of growth of each tested cell line following treatment with various concentrations of those compounds, and percentages of the results relative to the values of the untreated control cells are shown as the 50 % growth inhibitory concentration (GI_{50}), the 50 % lethal concentration (LC_{50}), and the total growth inhibition (TGI). However, this time, we concentrated on treating breast cancer.

Results demonstrated that the T-47D, HS 578 T, MDA-MB-231/ATCC, and MCF7 breast cancer cell lines were more responsive in dose-dependent manners to **18** (NSC784447) than to **20** (NSC784449). Two other cell lines, MDA-MB-468 and BT-549, were more responsive to **20** (NSC784449) treatment (Fig. 4).

Compound **20** showed higher activity against breast cancer (GI_{50} range of 1.13–2.81 μM) than compound **18** (GI_{50} range of 1.34–4.91 μM) (Fig. 5). These findings confirmed our initial screening findings and highlighted these potential compounds as potential future anticancer medications. Therefore, in this study, we aimed to characterize better and comprehend the biological actions of these two compounds.

3.3. *In-silico studies*

3.3.1. *Analysis of drug-likeness, absorption, distribution, metabolism and excretion (ADME), and toxicity parameters*

Synthesized compounds **5**, **17**, **18**, **19**, **20**, and **24** were analyzed using the SwissADME (Daina et al., 2017) and ADMETlab 2.0 tools

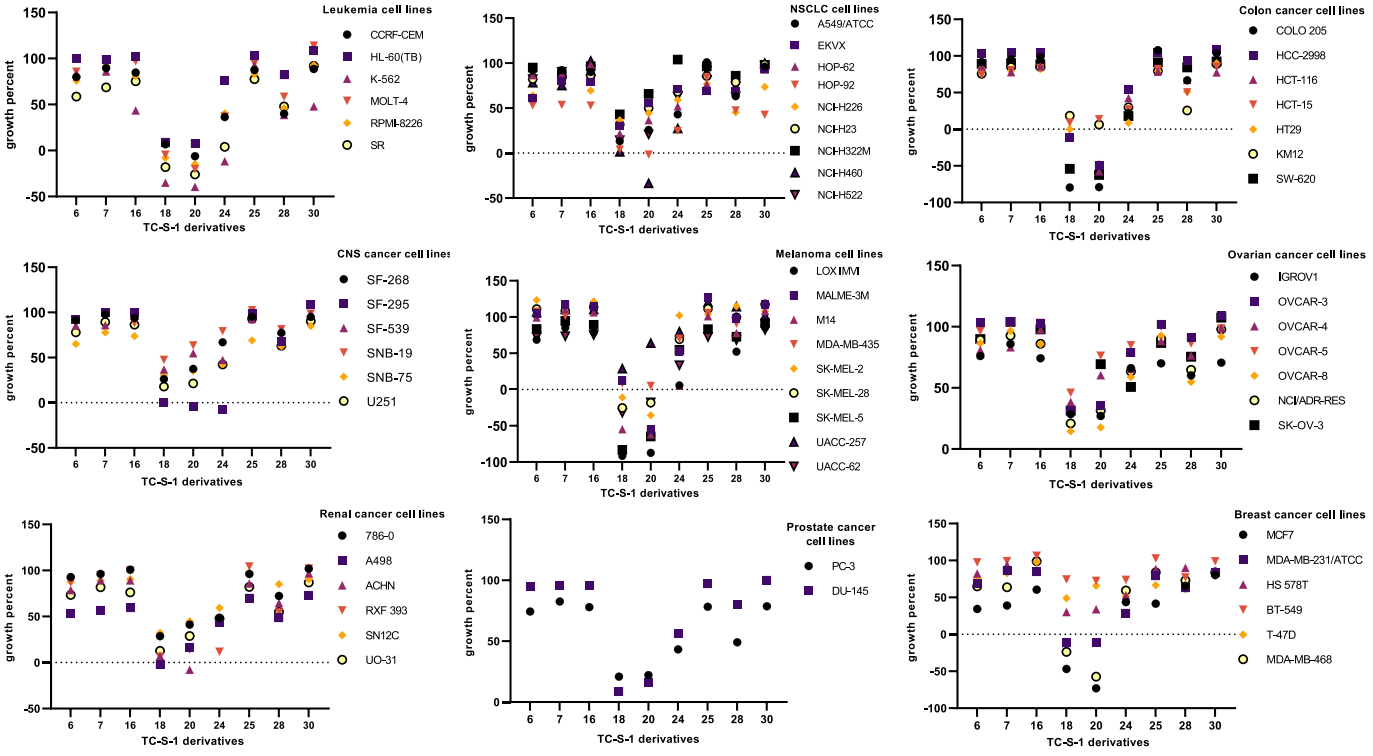

Fig. 3. Growth percentages of the NCI-60 human cancer cell lines after treatment with a single dose of 10 μM of each of our selected compounds **6** (NSC784437), **7** (NSC784438), **16** (NSC784445), **18** (NSC784447), **20** (NSC784449), **24** (NSC784440), **25** (NSC784442), **28** (NSC784441), and **30** (NSC784444).

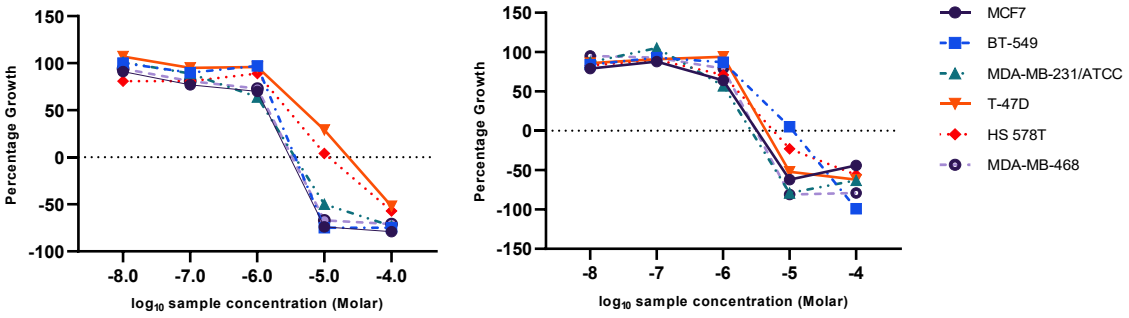

Fig. 4. Graphs illustrate the relationship between the dose and the effect of compounds **18** (NSC784447) and **20** (NSC784449) on breast cancer cell lines. A growth percentage value of 100 means that the cells grew at the same rate as untreated cells, while a value of 0 indicates no growth during the experiment, and a value of −100 signifies that all the cells were dead by the end of the experiment.

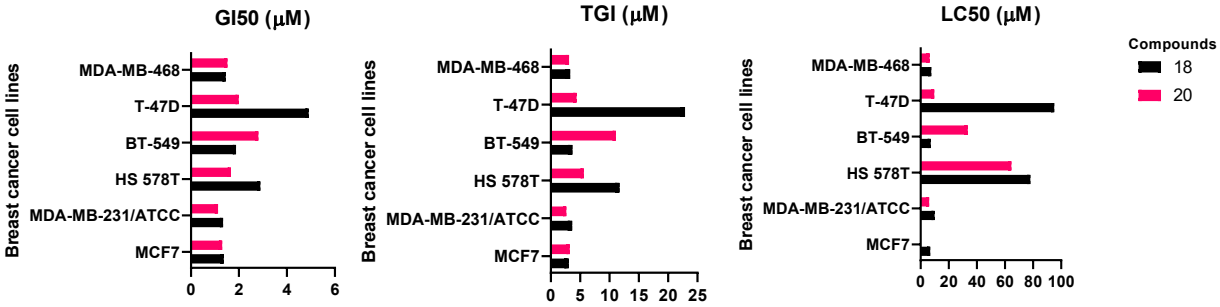

Fig. 5. Cytotoxic activities of **18** (NSC784447) and **20** (NSC784449) against breast cancer cell lines. GI_{50}, 50% growth inhibition; TGI, total growth inhibition; LC_{50}, 50% loss of cells.

(Xiong et al., 2021). These compounds met the criteria for drug properties as outlined by Lipinski's rule of five (Chen et al., 2020), Veber's rules (Yadav et al., 2021), and Ghose's rules (Morak-Młodawska et al., 2023). Log *p* values, which show the hydrophobicity or lipophilicity of a molecule, indicate that the compounds have acceptable values for absorption and permeability (Chen et al., 2023). The total polar surface area (TPSA), a measure of the polar surface area of a molecule, was also in a good range for oral bioavailability (TPSA values of < 140 Å) (Yukawa and Naven, 2020). The ADME analysis revealed that all of the compounds have the ability to be absorbed by the human intestine, and some even have the ability to cross the blood–brain barrier. Toxicity predictions showed that these compounds have no potential for carcinogenicity and a low risk for cardiotoxicity (Table 3, Table S3).

3.3.2. *Identification of drugs with similar profiles to our compounds by a COMPARE analysis*

The DTP-COMPARE analysis showed that **18** (NSC784447) and **20** (NSC784449) have antitumor characteristics that resembled those of investigated drugs and standard agents, with *p* values of 0.11–0.47 for **18** (NSC784447) and 0.21–0.52 for **20** (NSC784449). Table 4 presents the target descriptors, mechanisms, cell counts, and *p* values for the investigated drugs and standard agents.

Table 4
Investigated drugs and standard anticancer agents that share similar anticancer fingerprints and mechanistic correlations with **18** (NSC784447) and **20** (NSC784449).

Compound	Investigational drug					Standard agent				
	Rank	*r*	CCLC	Target descriptor	Mechanism	Rank	*r*	CCLC	Target descriptor	Mechanism
18 (NSC784447)	1	0.47	59	Anlotinib	RTK inhibitor	1	0.17	58	Mitindomide	Topo II inhibitor
	2	0.41	58	CT-XL228	Bcr-Abl inhibitor	2	0.16	58	Aclacinomycin	Topo I and II inhibitor
	3	0.40	50	AMG900	AURKA inhibitor	3	0.16	59	Echinomycin	HIF1 inhibitor
	4	0.37	56	Alisertib	AURKA inhibitor	4	0.15	41	Maytansine	Tubulin inhibitor
	5	0.36	59	Flavopiridol	CDK inhibitor	5	0.15	58	ICRF-159	Topo II inhibitor
	6	0.36	56	AZD-4205	JAK inhibitor	6	0.14	59	Thioguanine	PARP inhibitor
	7	0.34	56	X396	ALK inhibitor	7	0.13	59	Carboplatin	PARP inhibitor
	8	0.31	59	Foretinib	MET inhibitor	8	0.13	49	Menogaril	Topo II inhibitor
	9	0.31	59	Bafetinib	Bcr-Abl inhibitor	9	0.11	58	ICRF-187	Topo II inhibitor
	10	0.29	59	Danusertib	AURKA inhibitor	10	0.11	59	VP-16	Topo II inhibitor
20(NSC784449)	1	0.52	58	XR-11576	Topo I and II inhibitor	1	0.50	58	Amonafide	Topo II inhibitor
	2	0.49	59	Narazaciclib	CDK4/6 inhibitor	2	0.50	58	Pyrazoloacridine	HER2 inhibitor
	3	0.48	58	XR-5000	Topo I and II inhibitor	3	0.44	58	ICRF-187	Topo II inhibitor
	4	0.46	51	AS-703569	AURKA inhibitor	4	0.44	49	Deoxydoxorubicin	Topo II inhibitor
	5	0.46	56	XL-019	JAK inhibitor	5	0.43	58	Menogaril	Topo II inhibitor
	6	0.45	58	CT-XL228	Bcr-Abl inhibitor	6	0.37	59	Doxorubicin	Topo II inhibitor
	7	0.43	56	Alisertib	AURKA inhibitor	7	0.33	56	Tamoxifen	Nonsteroidal agent
	8	0.43	57	Pamiparib	PARP1/2 inhibitor	8	0.30	59	5-fluorouracil	cell-cycle inhibitor
	9	0.41	59	Vosaroxin	Topo I and II inhibitor	9	0.28	58	Etoposide	Topo II inhibitor
	10	0.31	57	Pacritinib	JAK inhibitor	10	0.21	58	Topotecan	Topo I inhibitor

Interestingly, our analysis of correlation patterns of 20 (NSC784449) correlated with amonafide, ICRF-187, deoxydoxorubicin, menogaril, and doxorubicin, which have been mechanistically reported to exhibit anticancer activities via TOPO II inhibition. Compound 18 (NSC784447), on the other hand, shared similar ($r = 0.11–0.17$) standard agent fingerprints with known inhibitors of TOPO II, such as mitindomide, ICRF-159, menogaril, ICRF-187, and VP-16. However, the investigated drug fingerprints showed the highest correlations in both **18** (NSC784447) and **20** (NSC784449) with multiple mechanisms of action, such as inhibition of AURKA, Janus kinase (JAK), cyclin-dependent kinase 4/6 (CDK4/6), poly(ADP ribose) polymerase 1/2 (PARP1/2), and receptor tyrosine kinase (RTK) ($r = 0.41–0.52$).

3.3.3. *Molecular modeling*

Etoposide, topotecan, ICRF-187, and doxorubicin have molecular structures similar to those of compounds **18** (NSC784447) and **20** (NSC784449) and are powerful inhibitors of TOPO I and II by interfering with TOPO-DNA complexes, resulting in DNA damage and cell death (Bali et al., 2018; Li et al., 2017; Marinello et al., 2018). Notably, amine-substituted derivatives of anthra[2,1–c] [1,2,5]thiadiazole-6,11-dione showed strong TOPO I inhibitory effects (Ali et al., 2021), indicating that our compounds might have related activities.

To investigate whether our series of compounds are potential inhibitors, compounds **18** (NSC784447) and **20** (NSC784449) were docked in predicted active target sites, including AURKA, CDK4, CDK6, TOPO I, and TOPO II. They exhibited binding energies ranging from −6.1 to −8.8 kcal/mol and interacted with neighboring amino acid residues (Table 5). Ligand-protein binding interactions are illustrated in 2D and 3D figures (Fig. 6).

The highest binding score was for compound 18 (NSC784447), with a binding score of −8.8 to TOPO I, followed by other proteins, including TOPO II, AURKA, and CDK4, with respective binding scores of −8.6, −8.5, and −8.1. In contrast, compound 20 (NSC784449) showed the highest binding score to the same proteins as compound 18 (NSC784447), such as TOPO I, TOPO II, AURKA, and CDK4, with respective binding scores of −8.7, −7.3, −8.4, and −7.4. The binding affinities were consistent with the observed cytotoxic activities and IC_{50} values, indicating that the binding of compounds to TOPO I was strongly associated with their cytotoxic activities. However, a few exceptions were observed.

4. Conclusions

In summary, a computational fragment-based drug discovery (FBDD) approach to develop and synthesize 26 compounds of tetraheterocyclic derivatives based on the 6H-thiochromeno[2,3–c]quinoline-12(12H)-one scaffold. This particular scaffold was selected because of its adaptability and distinctive moieties for medicinal applications, particularly in targeting DNA topoisomerases, which play a key role in addressing the demand for new anticancer drugs in breast cancer therapy. We investigated their cytotoxic and biochemical activities as multitarget small-molecule inhibitors through experiments involving two human breast cancer cell lines (MCF-7 and MDA-MB-468) and a panel of NCI-60 cancer cell lines. Structure-activity relationship (SAR) studies revealed that primary amine substitutions had stronger anticancer activity than secondary or tertiary amine substitutions. Compounds 5, 17, 18, 19, 20, and 24 showed promising cytotoxicity profiles against breast cancer cell lines. Computational analysis indicated that the synthesized compounds exhibited drug-like properties, with acceptable log P values, polar surface areas (TPSA), and the potential for intestinal absorption. The compounds demonstrated no potential for carcinogenicity and low risk of cardiotoxicity.

Further, we aimed to understand the mechanisms of action of our compounds by performing in-silico studies using a COMPARE analysis and molecular modeling experiments.

Overall, the study presents a promising series of compounds with potential multitarget anticancer properties, particularly in breast cancer treatment. The compounds showed favorable drug-like properties and demonstrated significant cytotoxicity against breast cancer cell lines. These findings suggest that compounds 18 (NSC784447) and 20 (NSC784449) warrant further investigation as potential anticancer agents. The work contributes to the development of novel drugs for cancer therapy and underscores the importance of interdisciplinary approaches that combine chemistry, biology, and computational modeling in drug discovery.

Table 5
Comparative docking profile of NSC784447 and NSC784449 against multiple targets.

Protein	18 (NSC784447)			20 (NSC784449)		
	ΔG = (kcal/mol)	Type of interaction	Interacting AA (distance (Å))	ΔG = (kcal/mol)	Type of interaction	Interacting AA (distance (Å))
AURKA	−8.5	Pi-Alkyl	LEU:139 (3.98)ALA:273 (4.43)	−8.4	Pi-Alkyl	LEU:139 (3.94)ALA:273 (4.31)
		H-Bond	GLU:260 (2.65)		H-Bond	GLU:260 (2.72)GLY:145 (2.20)
		Pi-Sigma	LEU:263 (3.76)		Pi-Sigma	LEU:263 (3.72)
CDK4	−8.1	H-Bond	ASP:158 (3.22)	−7.4	H-Bond	LYS:35 (2.62)ILE:12 (1.86; 4.95; 5.14)
		Pi-Anion	GLU:144 (4.99)		C–H-Bond	THR:102 (3.66)
		Pi-Alkyl	VAL:20 (5.28)LEU:147 (4.58)		Pi-Alkyl	LEU:147 (4.91)VAL:20 (4.65)
CDK6	−6.6	H-Bond	LEU:281 (2.29)	−6.1	H-Bond	LYS:279 (2.56)
		C–H-Bond	GLY:236 (3.53)ILE:235 (3.58)		C–H-Bond	THR:282 (3.48; 3.70)PHE:283 (2.85)
		Pi-Sigma	LEU:278 (3.72)		Pi-Cation	LYS:287 (3.73;5.27;5.05)
TOPO I	−8.8	H-Bond	DG:6 (2.29)DA:7 (2.37)	−8.7	H-Bond	DA:114 (1.93; 4.67; 2.25)
		C–H-Bond	GLN:421 (3.47)GLY:422 (3.54)		C–H-Bond	ILE:424 (3.14)
		Pi-Alkyl	LYS:493 (5.08)		Pi-Sigma	DT:116 (3.42; 5.89)
TOPO II	−8.6	H-Bond	ASN:779 ARG:929	−7.3	H-Bond	ARG:727 (2.56)GLU:712 (2.33)
		C–H-Bond	SER:778 GLY:777		C–H-Bond	GLY:1007 (3.37)
		Pi-Anion	DG:10		Pi-Anion	GLU:839 (4.22; 4.43)

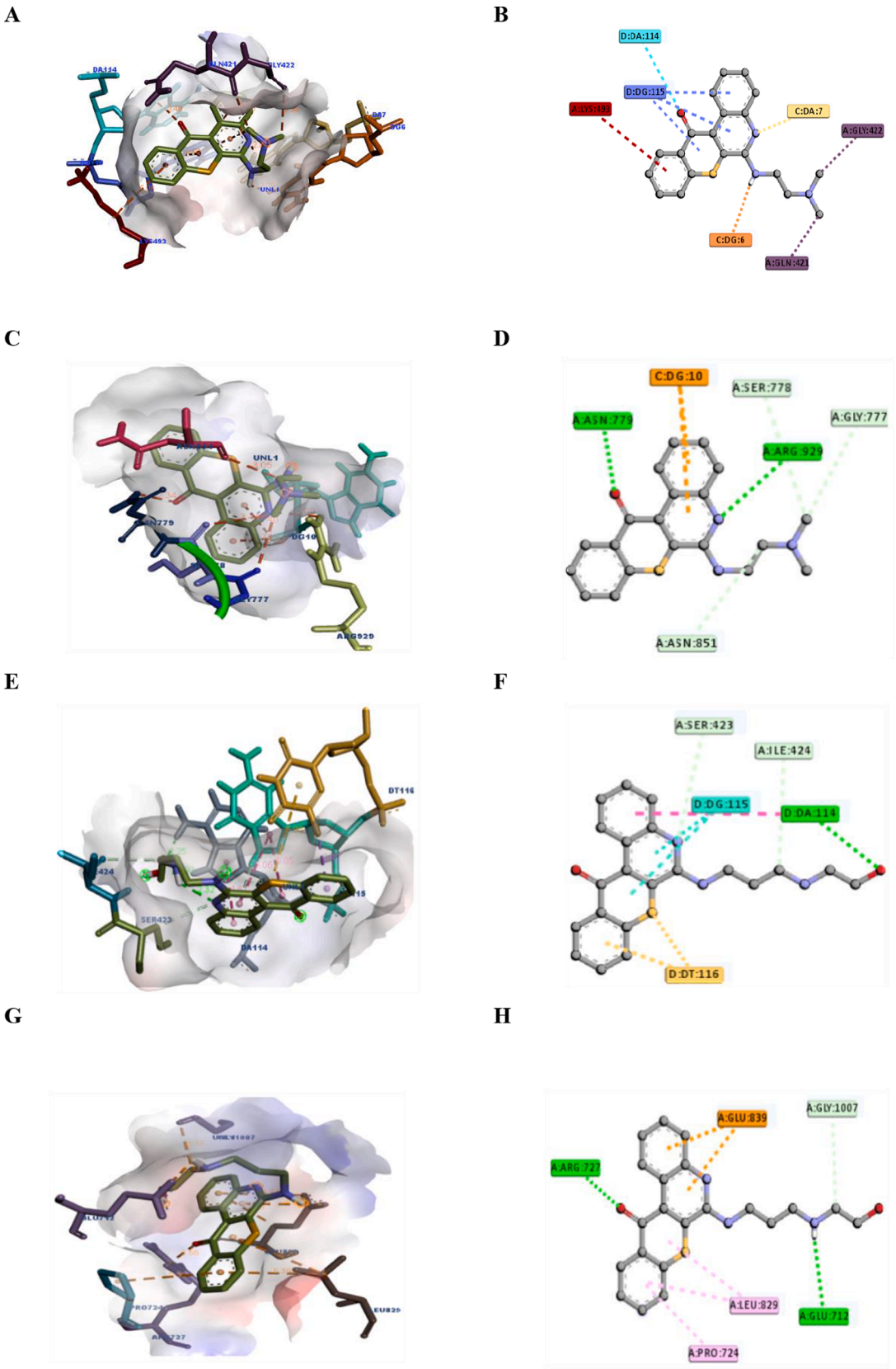

Fig. 6. Binding interactions of compounds **18** and **20** at topoisomerase (TOPO) I and TOPO II active sites. (**A**) 3D structures of **18** and the TOPO I (PDB ID: 1EJ9) receptor and distances (left). (**B**) 2D analysis of the amino acids and bonding interactions within the complex formed by **18** and TOPO I using Discovery Studio software. (**C**) 3D structures of **20** and the TOPO II (PDB ID: 4FM9) receptor and distances (left). (**D**) 2D analysis of the amino acids and bonding interactions within the complex formed by **20** and TOPO II using Discovery Studio software.

Declaration of competing interest

The authors declare that they have no known competing financial interests or personal relationships that could have appeared to influence the work reported in this paper.

Acknowledgments

The authors thank the NCI Developmental Therapeutics Program (DTP) for the 60-cancer-cell-line screening of selected compounds described in this paper, funded by the National Cancer Institute and National Institutes of Health (NIH-NCI).

Funding

The National Science and Technology Council, Taiwan (NSTC112-2314-B-038-006) and the Shin Kong Wu Ho-Su Memorial Hospital (SKH-TMU-112-02) awarded to H.-S. Huang. ATH Wu was also funded by Taipei Medical University (TMU111-AE2-I14-3) and the National Science and Technology Council (112-2314-B-038 -019-).

Appendix A. Supplementary material

Supplementary data to this article can be found online at https://doi.org/10.1016/j.arabjc.2023.105423.

References

Abdella, A.M., et al., 2020. Synthesis of heterocyclic compounds via Michael and Hantzsch reactions. J. Heterocycl. Chem. 57 (4), 1476–1523.
Abdolmohammadi, S., et al., 2020. Aqueous-Mediated green synthesis of novel spiro [indole-quinazoline] derivatives using kit-6 mesoporous silica coated Fe3O4 nanoparticles as catalyst. J. Heterocycl. Chem. 57 (7), 2729–2737.
Ali, A.A.A., et al., 2016. Novel Anthra[1,2-c][1,2,5]thiadiazole-6,11-diones as promising anticancer lead compounds: Biological evaluation, characterization & molecular targets determination. PLoS One 11 (4), e0154278.
Ali, A.A.A., et al., 2021. Structure-based strategies for synthesis, lead optimization and biological evaluation of N-substituted anthra[1,2-c][1,2,5]thiadiazole-6,11-dione derivatives as potential multi-target anticancer agents. Arab. J. Chem. 14 (2), 102884.
Bakır, T.K., Lawag, J.B., 2020. Preparation, characterization, antioxidant properties of novel Schiff bases including 5-chloroisatin-thiocarbohydrazone. Res. Chem. Intermed. 46 (5), 2541–2557.
Bali, S.K., et al., 2018. Activity of topotecan toward the DNA/topoisomerase I complex: A theoretical rationalization. Biochemistry 57 (9), 1542–1551.
Chen, T.-C., et al., 2019. Synthesis and biological evaluation of anthra [1, 9-cd] pyrazol-6 (2H)-one scaffold derivatives as potential anticancer agents. Arab. J. Chem. 12 (8), 2864–2881.
Chen, C.-L., et al., 2019. Synthesis and evaluation of new 3-substituted-4-chloro-thioxanthone derivatives as potent anti-breast cancer agents. Arab. J. Chem. 12 (8), 3503–3516.
Chen, X., et al., 2020. Analysis of the physicochemical properties of acaricides based on Lipinski's rule of five. J. Comput. Biol. 27 (9), 1397–1406.
Chen, Y.-F., et al. *In Vitro and In Silico Biological Studies of 4-Phenyl-2-quinolone (4-PQ) Derivatives as Anticancer Agents*. Molecules, 2023. **28**, DOI: 10.3390/molecules28020555.
Cho, Y.S., et al., 2010. 4-(Pyrazol-4-yl)-pyrimidines as Selective Inhibitors of Cyclin-Dependent Kinase 4/6. J. Med. Chem. 53 (22), 7938–7957.
Chokkar, N., et al., 2019. A Review on Quinoline Derived Scaffolds as Anti-HIV Agents. Mini Rev. Med. Chem. 19 (6), 510–526.
Daina, A., Michielin, O., Zoete, V., 2014. iLOGP: A Simple, Robust, and Efficient Description of n-Octanol/Water Partition Coefficient for Drug Design Using the GB/SA Approach. J. Chem. Inf. Model. 54 (12), 3284–3301.
Daina, A., Michielin, O., Zoete, V., 2017. SwissADME: a free web tool to evaluate pharmacokinetics, drug-likeness and medicinal chemistry friendliness of small molecules. Sci. Rep. 7, 42717.
Daina, A., Michielin, O., Zoete, V., 2017. SwissADME: a free web tool to evaluate pharmacokinetics, drug-likeness and medicinal chemistry friendliness of small molecules. Sci. Rep. 7 (1), 42717.
Day, P.J., et al., 2009. Crystal structure of human CDK4 in complex with a D-type cyclin. Proc. Natl. Acad. Sci. 106 (11), 4166–4170.
Dong, J., et al., 2018. ADMETlab: a platform for systematic ADMET evaluation based on a comprehensively collected ADMET database. J. Cheminf. 10 (1), 29.
Eberhardt, J., et al., 2021. AutoDock Vina 1.2.0: New Docking Methods, Expanded Force Field, and Python Bindings. J. Chem. Inf. Model. 61 (8), 3891–3898.
El Rhabori, S., et al., 2022. Design of novel quinoline derivatives as antibreast cancer using 3D-QSAR, molecular docking and pharmacokinetic investigation. Anticancer Drugs 33 (9), 789–802.
Fares, J., et al., 2023. Metixene is an incomplete autophagy inducer in preclinical models of metastatic cancer and brain metastases. J. Clin. Invest.
Ghanbari-Movahed, M., et al., 2021. Recent advances in improved anticancer efficacies of camptothecin nano-formulations: A systematic review. Biomedicines 9 (5).
Haji, N., et al., 2023. Heterocyclic Iminoquinones and Quinones from the National Cancer Institute (NCI, USA) COMPARE Analysis. Molecules 28 (13).
Marcus D Hanwell, D.E.C., David C Lonie, Tim Vandermeersch, Eva Zurek and Geoffrey R Hutchison, *Avogadro: An advanced semantic chemical editor, visualization, and analysis platform.* Journal of Cheminformatics, 2012. **4**: p. 17.
Hevener, K., et al., 2018. Recent developments in topoisomerase-targeted cancer chemotherapy. Acta Pharm. Sin. B 8 (6), 844–861.
Iqbal, J., et al., 2019. Exploration of quinolone and quinoline derivatives as potential anticancer agents. Daru 27 (2), 613–626.
Jaeckle, K.A., et al., 2020. Intra-CSF topotecan in treatment of breast cancer patients with leptomeningeal metastases. Cancer Med. 9 (21), 7935–7942.
Jampilek, J., 2019. Heterocycles in medicinal chemistry. Molecules 24 (21), 3839.
Karthikeyan, S., et al., 2023. A review on medicinally important heterocyclic compounds and importance of biophysical approach of underlying the insight mechanism in biological environment. J. Biomol. Struct. Dyn. 1–21.
Komatsu, H., et al., 2023. Three-component synthesis of quinoline-4-carboxylic acids based on doebner hydrogen-transfer reaction. J. Org. Chem. 88 (17), 12816–12820.
Kurniawan, Y.S., et al., 2021. An update on the anticancer activity of xanthone derivatives: A review. Pharmaceuticals (Basel) 14 (11).
Lauria, A., et al., 2021. Quinoline anticancer agents active on DNA and DNA-interacting proteins: From classical to emerging therapeutic targets. Eur. J. Med. Chem. 220, 113555.
Lawal, B., et al., 2021. Pharmacoinformatics and Preclinical Studies of NSC765690 and NSC765599, Potential STAT3/CDK2/4/6 Inhibitors with Antitumor Activities against NCI60 Human Tumor Cell Lines. Biomedicines 9 (1).
Li, F., et al., 2017. Camptothecin (CPT) and its derivatives are known to target topoisomerase I (Top1) as their mechanism of action: Did we miss something in CPT analogue molecular targets for treating human disease such as cancer? Am. J. Cancer Res. 7 (12), 2350–2394.
Lima, R.T., et al., 2018. The Antitumor Activity of a Lead Thioxanthone is Associated with Alterations in Cholesterol Localization. Molecules 23 (12).
Liu, Z., et al., 2020. Small molecule STAT3 inhibitor, 6Br-6a suppresses breast cancer growth in vitro and in vivo. Biomed. Pharmacother. 121, 109502.
Marinello, J., Delcuratolo, M., Capranico, G., 2018. Anthracyclines as topoisomerase II poisons: From early studies to new perspectives. Int. J. Mol. Sci. 19 (11), 3480.
Martins-Teixeira, M.B., Carvalho, I., 2020. Antitumour anthracyclines: Progress and perspectives. ChemMedChem 15 (11), 933–948.
Martorana, A., et al., 2022. Antiproliferative activity predictor: A new reliable in silico tool for drug response prediction against NCI60 panel. Int. J. Mol. Sci. 23 (22), 14374.
McIntyre, P.J., et al., 2017. Characterization of three druggable hot-spots in the aurora-A/TPX2 interaction using biochemical, biophysical, and fragment-based approaches. ACS Chem. Biol. 12 (11), 2906–2914.
McKie, S.J., Neuman, K.C., Maxwell, A., 2021. DNA topoisomerases: Advances in understanding of cellular roles and multi-protein complexes via structure-function analysis. Bioessays 43 (4), 2000286.
Min, H.Y., Lee, H.Y., 2022. Molecular targeted therapy for anticancer treatment. Exp. Mol. Med. 54 (10), 1670–1694.
Morak-Młodawska, B., et al., 2023. Study of Lipophilicity and ADME Properties of 1,9-Diazaphenothiazines with Anticancer Action. Int. J. Mol. Sci. 24 (8).
Orrantia-Borunda, E., et al., *Subtypes of Breast Cancer*, in *Breast Cancer*, H.N. Mayrovitz, Editor. 2022, Exon Publications Copyright: The Authors.; The authors confirm that the materials included in this chapter do not violate copyright laws. Where relevant, appropriate permissions have been obtained from the original copyright holder(s), and all original sources have been appropriately acknowledged or referenced.: Brisbane (AU).
Raevsky, O.A., et al., 2018. Applications of multi-target computer-aided methodologies in molecular design of CNS drugs. Curr. Med. Chem. 25 (39), 5293–5314.
Redinbo, M.R., Champoux, J.J., Hol, W.G.J., 2000. Novel insights into catalytic mechanism from a crystal structure of human topoisomerase I in complex with DNA. Biochemistry 39 (23), 6832–6840.
Schrödinger, L., & DeLano, W., *Pymol*. 2020.
Senerovic, L., et al., 2020. Quinolines and quinolones as antibacterial, antifungal, anti-virulence, antiviral and anti-parasitic agents. Adv. Exp. Med. Biol. 1282, 37–69.
Siegel, R.L., et al., 2023. Cancer statistics, 2023. CA Cancer J. Clin. 73 (1), 17–48.
Tang, L., et al., 2018. Genetic association between HER2 and ESR2 polymorphisms and ovarian cancer: a meta-analysis. Onco Targets Ther. 11, 1055–1066.
Trott, O., Olson, A.J., 2010. AutoDock Vina: Improving the speed and accuracy of docking with a new scoring function, efficient optimization, and multithreading. J. Comput. Chem. 31 (2), 455–461.
Wang, J., et al., 2020. The Impact of Chemotherapy Completion on the Efficacy of Irinotecan in the Preoperative Chemoradiotherapy of Locally Advanced Rectal Cancer: An Expanded Analysis of the CinClare Phase III Trial. Clin. Colorectal Cancer 19 (2), e58–e69.
Wendorff, T.J., et al., 2012. The Structure of DNA-Bound Human Topoisomerase II Alpha: Conformational Mechanisms for Coordinating Inter-Subunit Interactions with DNA Cleavage. J. Mol. Biol. 424 (3), 109–124.

Xiong, G., et al., 2021. ADMETlab 2.0: an integrated online platform for accurate and comprehensive predictions of ADMET properties. Nucleic Acids Res. 49 (W1), W5–W14.
Yadav, R., et al., 2021. Virtual screening, ADMET prediction and dynamics simulation of potential compounds targeting the main protease of SARS-CoV-2. J. Biomol. Struct. Dyn. 39 (17), 6617–6632.
Yuan, Y., Pei, J., Lai, L., 2020. LigBuilder V3: A multi-target de novo drug design approach. Front. Chem. 8.
Yukawa, T., Naven, R., 2020. Utility of physicochemical properties for the prediction of toxicological outcomes: Takeda perspective. ACS Med. Chem. Lett. 11 (2), 203–209.
Zhong, L., et al., 2021. Small molecules in targeted cancer therapy: advances, challenges, and future perspectives. Signal Transduct. Target. Ther. 6 (1), 201.